Fabrication and characterization of various engineered nanomaterials

A Mtibe[1*], TH Mokhothu[1*], MJ John[1,2], TC Mokhena[3], MJ Mochane[3]

[1]*CSIR Materials Science and Manufacturing, Polymers and Composites Competence Area, Nonwovens and Composites Research Group, Summerstrand, Port Elizabeth 6000, South Africa.*

[1,2]*Department of Chemistry, Faculty of Science, Nelson Mandela Metropolitan University, Port Elizabeth 6000, South Africa*

[3]*Department of Chemistry, University of Zululand, Kwadlangezwa 3886, South Africa*

[*]*Corresponding author Email, AMtibe@csir.co.za*

Abstract

In recent years, there has been growing demand of utilizing nanomaterials to develop new sustainable products. Nanomaterials offer unique extraordinary properties such as high surface area, eco-friendliness and good mechanical and physical properties. At the moment, the most promising nanomaterials that are widely used are nanoclay, carbonaceous (carbon nanotubes and graphene) nanomaterials, nanocellulose and metallic oxide nanomaterials. This chapter focusses on the fabrication methods of nanomaterials and their characterization as well as challenges involved during preparation. This encourages the development of innovative methods and technologies of engineering nanomaterials and possible scaling up of those technologies on an industrial scale. In addition to the milestone reached in the fabrication methods of nanomaterials, the future prospects in preparation processes as well as the main obstacles for their industrial scaling up have also been addressed in this chapter.

Keywords: Nanomaterials, Fabrication methods, Characterization, Industrial scale up

9.1 Introduction

In the past decades, the emergent technologies particularly nanotechnology were found to be potential in wider range of applications such as biomedical, packaging and electronics. Nanotechnology has been a research hotspot and its interest is growing considerable. This technology is defined as a science or technology that allows the manipulation of materials measuring 100 nm or less at least in one dimensions (Kamel 2007; Jonoobi et al. 2015). Given the smaller sizes together with good physical, chemical and mechanical properties of nanomaterials, nanomaterials showed superior properties in comparison to bulk materials counterparts (Jonoobi et al. 2015). The size, shape and morphologies of nanomaterials

determine their properties. However, the majority of studies are now focusing on controlling those parameters (Sirelkhatim et al. 2015). Nanomaterials may include carbonaceous materials such as carbon nanotubes and graphite, metal oxide nanoparticles, clay nanoparticles and nanocellulose.

Nanotechnology involves design, synthesis, characterization and applications of nanomaterials (Kamel 2007). Since the inception of nanotechnology, there have been thousands of publications, reviews, book chapters and patents highlighting the synthesis and characterization of nanomaterials. There are several methods available in the literature used to synthesize nanomaterials. For example, inorganic nanomaterials such as Metal oxides and nanoclays are synthesized by wet chemical, sol gel, chemical micro emulsion, hydrothermal, solvothermal, microwave assisted combustion, sono-chemical and direct precipitation (Elumalai and Velmurugan 2015). On the other hand, nanocellulose are prepared by acid hydrolysis, biological (enzyme treatment), mechanical and chemo-mechanical treatments (Satyamurthy et al. 2011; A Mtibe et al. 2015; Qing et al. 2013). In the case of carbonaceous nanomaterials, arc discharge, laser ablation and chemical vapour deposition techniques are widely used methods (Mubarak et al. 2014) but for graphene nano-sheets chemical, mechanical and thermal exfoliation techniques are used (Valapa, Pugazhenthi, and Katiyar 2015; Cooper et al. 2014; Zhang et al. 2005).

Due to the extraordinary properties of nanomaterials, many researchers are focussing on upscaling the production of nanomaterials (Jia and Wei 2017). However, the expansion of nanomaterials applications is the driving force for industrial production of nanomaterials. Moreover, the improvement in the mass production of nanomaterials may lead to cost reduction of the final product (Jia and Wei 2017).

Moreover, the current research is focussing on the synthesis of nanomaterials by using green methods (Goyal et al. 2017). Green methods involve the use of natural resource as a starting material and/or plant extracts in the case of metal oxides nanoparticles production as reducing agent. For example, Mokhena & Luyt 2017 prepared silver nanoparticles from chitosan, a stabilizing and reducing agent and use them to impregnate electrospun nanofibres. The synthesized silver nanoparticles showed antibacterial activity against both gram negative and gram positive. Furthermore, silver nanoparticles were believed to be non-toxic, biosafe and biocompatible with acceptable water vapour permeability within a range of required levels for treatment of injuries and wounds.

Interestingly, nanomaterials have also been utilized in composite field as reinforcement elements due to their extraordinary properties such as high aspect ratio, large surface area, high crystallinity, high mechanical properties and antimicrobial activity (Sirelkhatim et al. 2015; Jonoobi et al. 2015). In addition, nanomaterials are also used for protective coatings, thermal and electrical conductive materials, and in biomedical when antibacterial material is require (Landry et al. 2013; Mubarak et al. 2014; Salem et al. 2015).

In this book chapter we have extensively identified and discussed different types of nanomaterials, their synthetic approaches and characterization. In addition, nanomaterials which are discussed in this book chapter are characterized by the range of characterization techniques such as transmission electron microscopy (TEM), energy-dispersive X-ray (EDX), atomic force microscopy (AFM), scanning electron microscopy (SEM), X-ray diffraction analysis (XRD) and thermogravimetric analysis (TGA). In the subsequent sections, we also discussed both lab and industrial scale production of nanomaterials. The advantages and drawbacks of synthetic approaches are clearly highlighted in this study. This study also addresses the importance of using green methods to produce nanomaterials and also the upscaling of their production.

9.2. Overview of carbonaceous and their classification

9.2.1. Carbon nanotubes

Carbon nanotubes (CNTs) are one of the most fascinating nanomaterials in recent years owing to their unique properties such as high mechanical strength, large surface area, high thermal stability (>700 °C), high aspect ratio (length to diameter) and electrical conductivity which make them highly recommended for industrial applications (Ji et al. 2017). CNTs consist of a series of carbon atoms arranged in condensed benzene rings rolled into a uniform cylinder. These nanomaterials are classified into single and multiwall carbon nanotubes depending in the number of graphite layers. For example, single wall carbon nanotubes (SWNTs) consist of single layer of graphene sheet wrapped around to form a cylinder, while, multiwall carbon nanotubes (MWNTs) consist of two or several layers of concentrically nested cylinders. The properties and characteristics of CNTs are depicted in Table 1.

Table 1: Comparison between SWNTs and MWNTs properties (Singh et al. 2012).

SWNTs	MWNTs
Diameters range from 0.2 to 2 nm and lengths in microns	Diameters ranges from 1.4 to nearly 100 nm and lengths in several microns
Single graphene layer	Two or more graphene layers
Synthesis require catalyst	Can be synthesised without a catalyst
Difficult to perform bulk synthesis	Bulk synthesis is easy
More defects	Less defects
Poor purity	High purity
Easy characterization and evaluation	Difficult characterization and evaluation
Easily twisted	Difficult to twist

Various methods of producing CNTs have been documented in the literature and their efficiencies for mass production. The mass production of CNTs has been reported using chemical vapour deposition (CVD). Due to the unique properties of CNTs the demand of CNTs is growing day by day and therefore it requires large scale production to reduce costs. Moreover, the extensive research around the globe is ongoing to further improve the quality and the yield of CNTs.

9.2.1.1 Synthesis of carbon nanotubes

The synthesis of CNTs is generally carried out using different methods. These methods include: electric arc discharge, laser ablation and chemical vapour deposition. However, these methods are producing different types of CNTs with different properties. The synthesis of CNTs using these methods requires the carbon source, energy and metal catalyst. For example, in the case of CVD method the source of carbon is hydrocarbons such as methane in a gaseous state is heated in higher temperatures in the presence of catalyst to form CNTs.

9.2.1.1.1 Electric arc-discharge (AD)

This technique is one of the oldest methods used in synthesis of CNTs. It was pioneered by Iijima 1991. However, in this technique two graphite electrodes (carbon source) are placed close to each other about 1 mm in an inert gas of a pressure of 500 Torr. The electric discharge is employed as an energy source at an electric current of about 40-125 A and

potential difference of 20-50V. In addition, metal catalyst (cobalt, nickel, iron) and higher temperatures (2000-3000 °C) are required to evaporate the carbons from the graphite electrodes. The evaporated carbon is then condensed in the cathode thereby forming CNTs. The CNTs produced using this technique are normally short fibres with the diameter ranges from 0.6 to 1.2 nm.

For the production of MWNTs, the anode was graphite cylinder containing hexagonal boron nitride (h-BN) rod and pure graphite cathode were inserted inside the chamber. The inter-electrode gap was adjusted manually and the electric arc-discharge was produced between the electrodes in nitrogen atmosphere as shown in Figure 1.

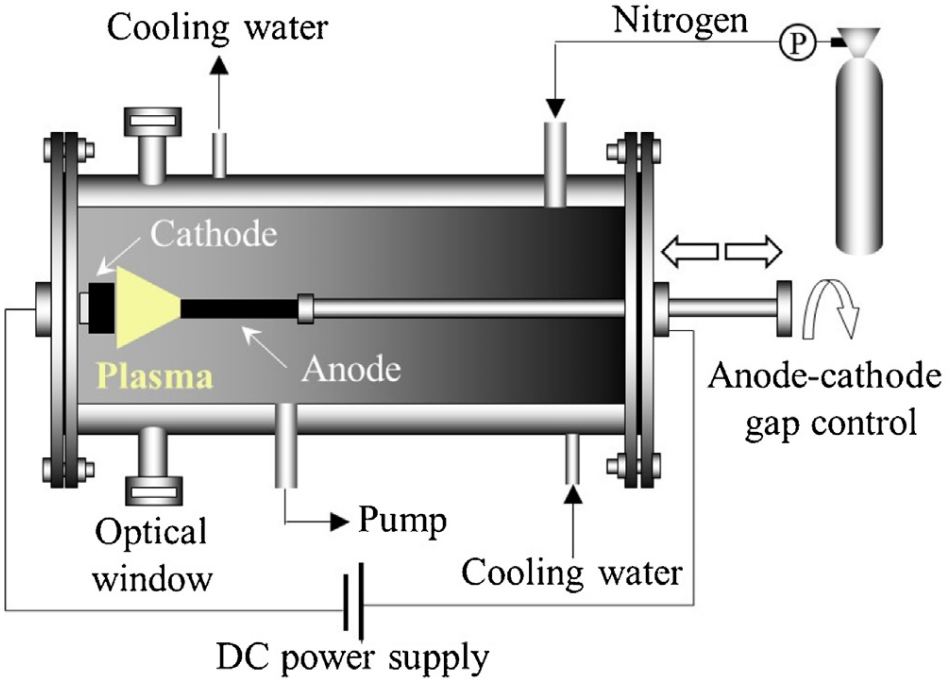

Figure 1 Schematic diagram of DC arc discharge reactor for production of CNTs adopted from (Belgacem et al. 2016)

The current which passes the electrodes created the plasma in between the electrodes. The ignition of plasma by contacting the electrode resulted in the rise in temperatures which led to the continuous evaporation of the material in the anode. The evaporated material was then deposited on the cathode. The diameters of MWNTs ranged from 20 to 30 nm and the lengths up to 1 μm. Similarly, SWNTs were produced by using the similar procedure and varying experimental parameters such as metal catalyst concentration, electrodes gap, current flow rate, temperature distribution and gas pressure (Fang et al. 2016)(Mubarak et al. 2014).

The major concern of AD is the low yield and quality of CNTs. Due to these reason, AD technique has not been successful for industrial scale up. Numerous authors are researching on the improvement of the yield and the quality of CNTs using AD. Among those authors, Zhao et al. 2006 suggested that the mass production (20-30%) of SWNTs can be achieved by adding 1 % of Fe catalyst in hydrogen (H_2) mixed with inert gas. The formation of SWNTs containing impurities was confirmed by energy-dispersive X-ray (EDX) and high resolution transmission electron microscopy (HRTEM). Furthermore, the authors purified SWNTs by refluxing them in hydrogen peroxide (H_2O_2) and subsequently rinsed with hydrochloric acid (HCl). This purification method was found to enhance the purity of SWNTs to be above 90%. The optimisation of pressure (100 to 700 Torr) of the inert gas to enhance the yield of CNTs was reported in another study (Kim and Kim 2006). The highest yield of CNTs was achieved by using 300Torr air pressure. The role of inert gas was to quench the carbon vapour, to achieve supersaturations followed by nucleation and the growth of CNTs. It was suggested that the use of atmospheric air could reduce the cost of the final product. Berkmans et al. 2015 and Su et al. 2014 also confirmed that CNTs can be produced using open air at low current densities.

Recently, Maria & Mieno 2015 employed a low-frequency biopolar pulsed arc discharge method with the aim to supress the carbon deposits and increase the production efficiency of CNTs. In this method, both electrodes have same diameters containing metal catalyst. However, carbon sublimate in both electrodes unlike in DC electric arc discharge. This technique displayed good production rate of SWNTs when the pulse frequency was increasing from 0.05 to 5 Hz.

9.2.1.1.2 Laser ablation

This technique applies similar principle like AD, but it uses laser pulses as a source of energy instead of heat. Studies showed that the quality and the yield of CNTs depend on laser power, catalyst and temperatures (Chernysheva et al. 2017)(Eatemadi et al. 2014). For example, when the laser power increase, the diameters of CNTs become thinner (Eatemadi et al. 2014). SWNTs produced by optimising the laser wavelength of 1064 or 355 nm in the fluence range of 1-6J.cm^{-2} were long with diameters of about 1.25 nm. Scanning electron microscopy (SEM) and scanning transmission electron microscope (STEM) also showed that the final product contained impurities of residual catalyst (Chrzanowska et al. 2015). The potential of

large production of SWNTs using KrF excimer laser ablation in nitrogen atmosphere was suggested in another study (Moise et al. 2015). The authors revealed that over 70% yield of SWNTs was produced (Moise et al. 2015). In another study the formation of SWNTs films by using a drop-and-dry method and irradiation with ultrafast femtosecond laser pulses was observed (Choi et al. 2016). The alignment of SWNTs was randomly oriented in the films.

Most recently, an innovative laser ablation chamber design consisting of longer ovens and longer cold finger has been developed to obtain CNTs (Bota et al. 2017). This chamber design uses KrF excimer laser, producing 25 ns pulses at 248 nm with 100–700 mJ pulse energy. Graphite cement (carbon source) and Pt and Co (catalyst) were mixed and subsequently heated at 800 °C to remove the unreacted resin and any other organic compounds. The ablation of pure graphite produced carbon nano-onions with diameters between 6 and 25 nm. On the other hand, the ablation of graphite in the presence of catalyst Pt-Co catalyst showed formation of SWNTs with diameters between 1.2 and 1.5 nm embedded within amorphous carbon. The formation of these nanomaterials was confirmed by Raman spectroscopy. The Raman spectrum displayed three major bands which were corresponding to SWNTs. The yield of SWNTs was estimated to be approximately 70%.

Disadvantages of Arc discharge and laser ablation are as follow:

1) These methods uses high amount of energy.
2) Require large amount carbon/graphite to form CNTs.
3) The CNTs contains unwanted amorphous carbon and catalysts. The removal of those contaminants requires costly purification processes.
4) Low yield.

Unfortunately, these disadvantages make these methods not economically viable for industrial scaling up.

9.2.1.1.3 Chemical vapour deposition (CVD)

This technique is widely used for large scale production of high quality and well oriented CNTs. The preparations of CNTs in CVD involves catalytic decomposition of hydrocarbons such as methane, ethylene and benzene on a nanolayer transition metal catalysts such as Ni, Co and Fe at higher temperatures (700-900 °C) to form CNTs. However, in some cases the combination of two metals can be used as a catalyst (Dunens, MacKenzie, and Harris 2010).

Similarly to previously discussed methods for the synthesis of CNTs, transition metal catalysts plays a magnificent role in CVD method to produce different types of CNTs, to improve the yield and the quality and to produce well oriented CNTs.

For large scale production of CNTs, fluidized bed chemical vapour deposition (FBCVD) has been studied. This method is reported to produce SWNTs capacity of 1000 kg per year with price lower than US $2000 per kg (Jia and Wei 2017). Dunens et al. 2010 produced double wall carbon nanotubes (DWNTs) by FBCVD system. The authors synthesized DWNTs at 850 °C using alumina (Al_2O_3) as a support of catalyst which consist of a mixture of Fe and Mo ratio 9:1 and methane as carbon source. About 200% yield of the product relative to the weight of the Fe:Mo/Al_2O_3 catalyst was obtained.

The research is now focusing on the modification of CVD using to improve growth rate, quality and yield and make the growth process more efficient. This modification systems include: aerosol-assisted (AACVD) (Meysami et al. 2015), plasma enhanced (PECVD) (Ji et al. 2017), hydrogen free spray pyrolysis (HSPCVD) (Ionescu et al. 2011), catalytic (CCVD) (Almkhelfe et al. 2017), low temperature (LTCVD) (Maruyama et al. 2017) and alcohol catalytic (ACCVD) (Hou et al. 2017). For example, AACVD and PECVD are capable of producing low cost and high efficient vertically aligned CNTs (Meysami et al. 2015; Ji et al. 2017).

There are new developments in the production of CNTs from plastic materials (Wu et al. 2014). Wu et al. 2014 synthesized CNTs from waste plastics (high density polyethylene (HDPE) and HDPE containing polyvinyl chloride (PVC)) using a reactor consists of two-stage fixed pyrolysis-reforming reaction system, where raw plastic was pyrolyzed in the first reactor. The vapour was transferred into the second stage where it was converted to CNTs in the presence of a metal catalyst. Most recently, Bajad et al. 2017 simultaneously produced liquid hydrocarbons, CNTs and hydrogen rich gas from post-consumer edible oilcans made up of HDPE using multi-core reactor. The authors revealed that MWNTs with the diameters 20-50 nm and average wall thickness of 10 nm were successfully produced. The results indicated that the increase in pyrolysis temperature from 450 to 700 °C led to the decrease in the yield of liquid hydrocarbons while, the CNTs yield increased with increase pyrolysis temperature. The CNTs yield of 6.03g per 30g of input material at 700 °C was achieved. The benefits of this innovative approach is the reduction of energy and capital cost.

The advantages of CVD are as follows:

1) Economically viable for large production of CNTs.
2) Produces high pure products.
3) Ease to operate.
4) Availability of raw material in the form of hydrocarbon gases and plastic waste.
5) It is versatile so it is possible to coat almost any shape and any size of material.
6) Other forms of CVD can produce vertically and horizontally aligned CNTs unlike other film making techniques.

9.2.2 Graphite nano-sheets

9.2.2.1 Exfoliation techniques for fabrication of graphite nano-sheets

Expandable graphite (EG) also commonly known as graphene, natural graphite (NG) or graphite is a single-layered two dimensional (2D) structure of carbon atoms covalently bounded together in the same plane with Van der Waals forces acting between consecutive layers (Uhl et al. 2005; Song et al. 2011; G. Zhang et al. 2016). Expandable graphite is regarded as one of the promising carbonaceous materials that has drawn attention for reinforcing polymer matrices due to its extraordinary electrical; thermal; mechanical; barrier and flame retardant properties. However, the critical challenge of using EG for reinforcing is the breaking down of the intercalated graphite layers that causes aggregation in polymer matrices. Several attempts to exfoliate graphite layers to expanded graphite or graphite nano-sheets have been investigated to achieve good dispersion and optimize the composites' performance. A detailed review on methods of graphite exfoliation has been reported by (Cai et al. 2012) addressing the importance of large scale production and application of exfoliated graphite materials with controlled properties. Several exfoliation techniques such as chemical or electrochemical (Malas, Pal, and Das 2014; Song et al. 2011; Pang et al. 2012; Hong, Wang, and Jin 2013), mechanical (Novoselov et al. 2005) and thermal and/or chemical (Valapa et al. 2015; Yasmin et al. 2006; Mochane & Luyt 2015a; Mochane & Luyt 2014b; Greco et al. 2012) have been the mostly utilized to break down the intercalated layers to achieve percolation and network formation within a polymer matrix. Furthermore, melt mixing is one of the mostly used preparation technique to disperse the expanded graphite layers in polymeric matrices and maximise their applications. In addition, X-ray diffraction

analysis (XRD) and scanning electron microscopy (SEM) are the mostly used analytical techniques for the identification of exfoliated graphite monolayers.

9.2.2.2 Mechanical exfoliation technique

Mechanical exfoliation or referred to as micromechanical cleavage is a popular method that has been explored for the separation of graphene and it is the first method of obtaining two-dimensional crystals. The graphene layers are separated by repeated peeling of a graphite crystal using scotch/adhesive tape. This was demonstrated by (Novoselov et al. 2004) achieving single layer graphene (SLG) using an adhesive tape. Multiple-layer graphene is cleaved into various flakes of few-layer graphene (FLG) and extensive rubbing of the graphite surface against a flat surfaces is another way to get multiple or even single atomic layers of graphite plates (Novoselov et al. 2005; Bonaccorso et al. 2012; Jayasena and Subbiah 2011). Exfoliation of graphene involves the use of an atomic force microscope (AFM) tip along with an array of highly ordered pyrolytic graphite (HOPG) mesas made from oxygen-plasma etching method. The HOPG islands are then transferred to a SiO_2/Si substrate through a wet or dry transfer technique (Lu et al. 1999). A variation of this method involves gluing a block of prepared graphite to an AFM tip and scratched on Si substrates (Zhang et al. 2005). However, it is difficult to control the separation and number of graphene layers generated using these mechanical methods. In addition, in order to realize these applications, scalable and cost effective production methods of graphene are essential. Detailed understanding of growth kinetics and production control is highly desired to prepare large-scale high quality exfoliated graphene. Recently (Zabihi et al. 2017) tailored graphite nano-platelets (GNP) grafted with maleic anhydride to be purposefully incorporated into epoxy polymer matrix as a potential industrial application. The maleic anhydride grafted graphite nano-platelets (*m*-GNP) were prepared by combining the kitchen blender approach and Diels-Alder chemistry, in which maleic anhydride was simultaneously used as stabilizing agent in "kitchen blender" approach and dieneophile in Diels-Alder cycloaddition reaction. They further used a recyclable process to change *m*-GNP to the highly-reactive GNP (*f*-GNP) which exhibits a strong affinity towards the epoxy polymer matrix. They reported that at low *f*-GNP (0.5 wt%) significant improvements in flexural strength (~65%) and tensile strengths(~54%) of epoxy nanocomposite was achieved. It is believed that this new protocol for functionalization of graphene nanomaterials will pave the way for relatively simple industrial scale fabrication of high performance graphene based nanocomposites.

9.2.2.3 Chemical or electrochemical exfoliation technique

Chemical exfoliation of graphite layers involves the oxidation of graphite with oxidants and strong acids based on Hummers, Staudenmaier and Brodie methods or by electrochemical oxidative exfoliation of bulk graphite to yield expanded graphite (EXG) or graphene oxide (GO) (Liu 2017; Cooper et al. 2014). Graphene/graphite sheets having oxygen functional groups facilitate the dispersion of the sheets in aqueous and organic solvents leading to increased yields of exfoliate. However, oxygen containing functional groups can decrease graphene's electronic conductivity, which cannot be completely restored upon further chemical reduction thereby losing the inherent advantages of graphite monolayer (Gómez-Navarro et al. 2007; Allen 2009; Wang et al. 2011). The method involves treating graphite with essentially a water-free mixture of chemicals such as concentrated sulfuric acid (H_2SO_4), sodium nitrate ($NaNO_3$) and potassium permanganate ($KMNO_4$) and the process requires less than two hours for completion at temperatures below 45° (Hummers et al. 1958). For instance, (Song et al. 2011) followed a typical Hummers method to prepare exfoliated graphene sheets reinforced polyethylene nanocomposites while (Kuila et al. 2012) modified the method by introducing dodecyl amine to prepare exfoliated graphite oxide (GO) reinforced polyethylene nanocomposites. In this case, the reflection peak of graphite oxide at 11.2° completely disappeared after surface modification due to the extensive intercalation and exfoliation of GO by dodecyl amine. In the case of graphene sheets prepared by (Song et al. 2011) the interlayer space of 0.34 nm for pristine graphite (26.5°) was increased up to 0.80 nm (11.0°) after oxidation due to the intercalation by oxygen containing groups. From both studies changes in the interlayer spacing and reflection peak of graphite/graphene were observed which suggested the exfoliation of graphite/graphene layers as a result of chemical exfoliation. However, the disadvantage with chemical exfoliation method is the utilization of hazardous chemicals (H_2SO_4, KMnO4, hydrazine and more) which are environmentally harmful and the production process is time-consuming.

9.2.2.4 Thermal and/or chemical exfoliation technique

Thermal exfoliation is a technique that involves rapid heating of expandable graphite which is believed to cause numerous small molecule species such as water, CO_2 and CO to evolve causing increasing in internal pressure, forcing the graphite sheets apart and resulting to

enormous increase in volume, high-surface area material with low bulk density and expansion thickness of about 80-100 times (Figure 2a expandable and Figure 2b expanded graphite). Furthermore, the exfoliation of graphite monolayers causes a sharp decrease in the peak intensity of the graphite peak (~ 26.2-26.55°) as shown from the XRD patterns in Figure 2c which suggests the exfoliation of graphite sheets. Several studies investigated the influence of thermal exfoliated graphite reinforced polymer composites (Valapa et al. 2015; Yasmin et al. 2006; Mochane & Luyt 2015a; Mochane & Luyt 2014b; Greco et al. 2012). Expanded graphite (EG) was subjected to different temperatures ranging from 200-1000°C to determine the optimum temperature of exfoliation based on the carbon yield (%) and bulk density (kg/cm^{-3}) by (Valapa et al. 2015) From their results, there was no significant deviation in the graphite peak (26.52°) for all expanded graphite samples subjected to XRD analysis (Figure 2d). However, the peak intensity gradually decreased with increased exfoliation temperatures when compared to EG and a significant decrease was observed up to 750°C. This was attributed to high levels of exfoliation due to the maximum swelling of intercalates that increased the interlayer distance between graphene sheets resulting in high volume of expansion up to 750°C. While above 750°C, the increased exfoliation temperatures caused the evaporation of intercalates as gaseous products such as CO_2 and SO_2 and lead to the reduction in the bulk density and sample expansion (Table 1). In this case it is clear that even though the least bulk density might correspond to a maximum increase in exfoliation rate, there other two factors such as carbon yield and the volume of exfoliation that should be taken into consideration for optimization of exfoliation temperature.

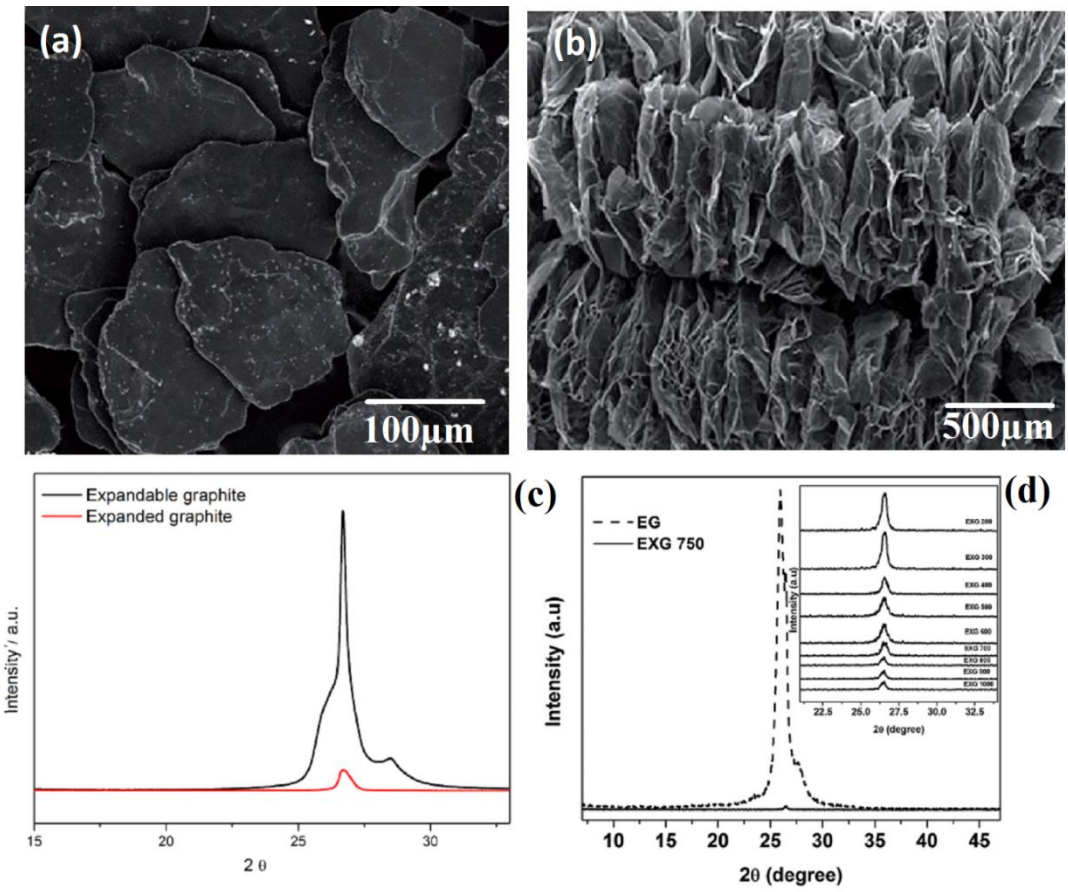

Figure 2 **SEM images of (a) expandable and (b) expanded graphite; XRD pattern of (c) expandable and expanded graphite and (d) expandable graphite (EG) and exfoliated graphite (EXG) Reprinted from (Valapa et al. 2015), Copyright 2015, with permission from Royal Society of Chemistry.**

Table 1 Effects of temperature on exfoliation of EG[a]. Reprinted from (Valapa et al. 2015), Copyright 2015, with permission from Royal Society of Chemistry.

Sample name	Volume exfoliated (mL)	Weight after exfoliation (g)	Bulk density (kg cm^{-3})	Carbon yield (%)
EXG 200	0.1	0.05	500	100
EXG 300	3	0.046	15.33	92
EXG 400	4.5	0.043	9.56	86
EXG 500	9	0.041	4.55	82
EXG 600	12.5	0.041	3.28	82
EXG 700	15	0.041	2.73	82
EXG 750	15.5	0.050	2.58	80

EXG 800	14	0.034	2.43	68
EXG 900	12	0.023	1.92	46
EXG 1000	4	0.007	1.75	14

[a] EXG 200 represents the EG exfoliated at 200°C.

On the other hand, (Greco et al. 2012) worked on the development of amorphous thermoplastic matrix nanocomposites based on graphite nanoparticles. The expanded graphite (GICe) was obtained by placing graphite interaction compound (GIC) into an oven at 700°C for 2 minutes to yielding a worm like structure (Figure 3). They reported that GIC reinforced nanocomposites showed moderate increase in electrical properties whereas GICe and GICes nanocomposites where well dispersed and showed significant improvement of the electrical conductivity. Furthermore, from their XRD results graphite showed two peaks at 26.55° and 26.05° attributed to non-intercalated graphite lamellae and intercalated lamellae respectively. After thermal treatment of GIC, the peak at 26.05 decreased for GICe samples which suggested the exfoliation of graphite intercalates but with the presence of intercalated graphite sheets (26.2°). This was attributed to the fact that the maximum temperature achieved during thermal exfoliation was lower than the end-set of dissociation of the expanding compound. Similarly was the case of (Mochane & Luyt 2015a) Mochane and Luyt (2015a**)** in the investigation of the synergistic effect of expanded graphite, diammonium phosphate and Cloisite 15A on flame retardant properties of EVA and EVA/wax phase-change blends. The expanded graphite was exfoliated enough to allow the wax chains to penetrate in between the graphite layers and slightly separated them, giving rise to smaller and better dispersed EG particles. Furthermore, the presence of expanded graphite in EVA and EVA/wax blend improved their thermal stability as well as significantly improved the flame resistance of the composites with the presence of Cloisite 15A and DAP.

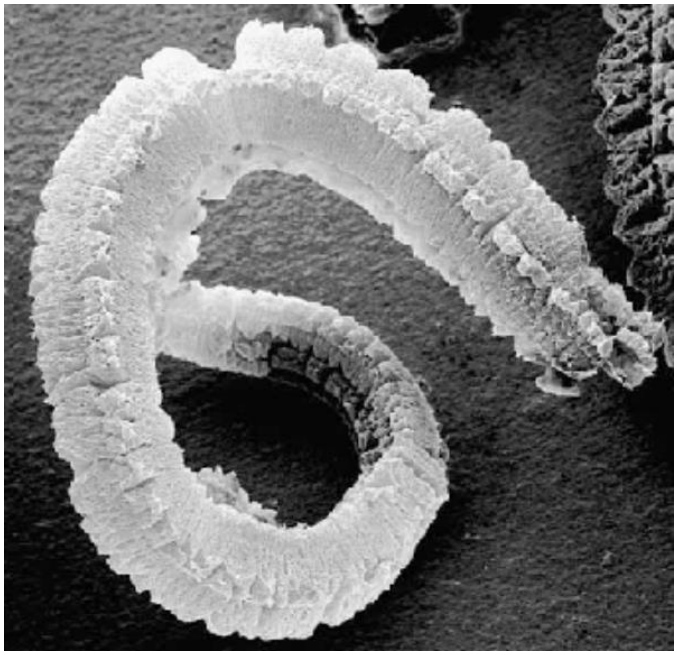

Figure 3 Worm like structure of thermally exfoliated graphite

Besides thermal exfoliation, a combination of chemical and thermal exfoliation has also been investigated to maximise the application of graphite. For instance, exfoliated graphite and its acrylonitrile butadiene styrene (ABS) composites prepared by chemical route and then further subjected to thermal oxidation and sonication for size reduction to increase the interlayer spacing in natural flake graphite was investigated (Neha et al. 2012). In this study, Staudenmaier method was used to prepare graphite oxide followed by heating in a muffle furnace set at 950°C for 30 seconds for reduction of GO. The thermal expansion was carried out to increase the interlayer spacing and further reduction in van der Waals forces. After thermal exfoliation the graphite peak at $2\theta = 26.4°$completely disappeared and the treatment resulted in size reduction and increase in interlayer spacing of exfoliated graphite which was confirmed from the XRD analysis. Furthermore, the incorporation of exfoliated graphite in ABS decreased the electrical resistivity value of the composites. The advantage of thermal exfoliation technique is that it's generally fast because of high temperature processing and exfoliation can occur within seconds. Furthermore, most thermal exfoliation methods produce graphene in a gaseous environment, therefore, the use of liquids is avoided. For some applications, such as electrodes in lithium batteries, dry graphene is required. When graphite oxide is used as the starting material, thermal exfoliation usually results in simultaneous exfoliation and reduction of graphene.

9.3 Synthesis of metal oxide nanoparticles

Synthesis of metal oxide nanoparticles using bio- and/or nanotechnology has received significant attention globally particularly due to their size (nanometre with particle sizes ranges between 1 and 100 nm), larger surface area, compositions, crystallinity and the shape. These characteristics of nanoparticles are very imperative to determine the properties of nanoparticles. The most commonly studied metal oxide nanoparticles are zinc oxide (ZnO), silica dioxide SiO_2), titanium dioxide (TiO_2), silver oxide (Ag_2O) nanoparticles and many more (Thakkar et al. 2010). These nanoparticles offer unique antifungal and antimicrobial, electrical conductivity, optical absorption, semiconducting and chemical sensing properties. The properties of nanoparticles together with their advantages such as nontoxic, biosafe, and biocompatible make them suitable candidates to be utilized in diverse applications such as biomedical, food packaging and agricultural. As the utilization of nanoparticles in these applications is expanding, the up scaling is required which will aid in the cost reduction of the final product. Numerous researchers have investigated the small scale production of nanoparticles using chemical, physical, green methods and the combination of these methods and some developments on up scaling have been reported as well (Shankar and Rhim 2017; Nagarajan and Kuppusamy 2013). Moreover, there has been a growing interest in the preparation of nanoparticles using plant extracts due to the availability of resources, cost-effectiveness, eco-friendly and can be easily scaled up (Nagarajan and Kuppusamy 2013).

9.3.1 Chemical synthesis

Precipitation is one of the widely used chemical synthesis approaches of metal oxide nanoparticles. In this method, the production of nanoparticles is achieved by mixing a low cost precursor and stabilizer. The role of stabilizer in this method is to prevent agglomeration of the particles and thus producing uniform particles. For examples, zinc nitrate hexahydrate as a precursor and starch as a stabilizer were used to synthesize zinc nanoparticles (Lanje et al. 2013). XRD results revealed that the synthesized zinc nanoparticles (zincite) were highly crystalline with hexagonal wurtzite type structure and high purity. The particle size of zincites was 40 nm measured by TEM which was higher than the crystallite size (19 nm) measured by XRD. Apart from zinc nitrate hexahydrate, other different precursors such as zinc acetate dehydrate and zinc nitrate were also investigated to prepare zinc nanoparticles

(Sharma and Ghose 2015; Saha et al. 2017). In a separate study, Shankar and Rhim 2017 simultaneously produced Zn nanoparticles, copper oxide nanoparticles and silver nanoparticles in a gram scale. The yield of Zn, copper and silver nanoparticles were 25.2%, 34.3% and 50%, respectively. SEM revealed that the shape of Zn nanoparticles were spherical with the sizes of 50-100 nm, whereas copper nanoparticles were rod-like shaped with the sizes of 100-200 nm. On the other hand, TEM revealed that silver nanoparticles were needle shaped with diameters ranges from 50-100 nm and the lengths ranges from 2-10 μm. It was also determined by XRD that all nanoparticles were highly crystalline and pure.

In the case of silver nanoparticles, the synthesis is usually carried out using polyol method where silver nitrate, ethanol and polyvinylpyrrolidone are used as a precursor, reducing agent and surfactant, respectively (Sedira et al. 2014). Sedira et al. 2014 reported that silver nanoparticles demonstrated antibacterial activity towards *E. coli* and *P. aeruginosa*. This was achieved by measuring Ag^+ release using acetic acid to increase the release. Recently, Saoud et al. 2015 proposed a hybrid approach of synthesising silver nanosphere on the surface of Zn nanorods by deposition precipitation method accompanied with microwave oven and subsequently irradiated for 10 minutes. TEM and FTIR confirmed that there was no chemical bond between Ag nanosphere and Zn nanorods but, the presence of Ag in the system improves the photocatalytic efficiency of Ag/Zn nanorods.

Chemical synthesis approach shows several disadvantages such as it requires labour extensive and time, costly, uses toxic chemicals, contamination from the precursor materials and also producing secondary wastes.

9.3.2 Physical and the combination of physical with chemical and green methods

Solvothermal is one the widely used method reported in the literature for synthesis of metal oxide nanoparticles. This method is a two-step process, where metal oxide nanoparticles are synthesised by chemical method followed by calcination. For instance, mesoporous Zn nanoparticles were synthesized by solvothermal method (Bijanzad et al. 2015). In this method, zinc coordination compound was formed by mixing zinc nitrate tetrahydrate and 2-aminonicotinic acid and subsequently calcined at 550 °C for 4 hours to produce zinc mesoporous nanoparticles. The resultant Zn mesoporous nanoparticles had surface area of 8.13 m^2/g, pore size of 22.6 nm and high photocatalytic activity. The reduction of calcined

temperature to 300 °C has resulted to larger specific surface area (about 21.4 m^2/g) (Sharma and Ghose 2015). In general, calcination was found to cause agglomeration of nanoparticles (Sharma and Ghose 2015).

Other authors synthesised metal oxide nanoparticles using one-pot synthesis approach. In this approach, seed extracts (a reducing agent) and a precursor were mixed together followed by calcination at 400 °C (B. Paul et al. 2017). Zn nanoparticles produced from this approach were used as catalyst for the synthesis of 2-benzimidazoles derivatives and sonocatalyst in the degradation of methylene blue (MB) and rhodamine B (RhB) dyes. Most recently, a novel green synthesis of Zn nanoparticles range from 30–80 nm using leaf extracts assisted with microwave heating (850 W, 60 s) was investigated (Salari et al. 2017). The authors also compared the synthesised Zn nanoparticles and zinc sulphate ($ZnSO_4$) (a precursor). The results showed that Zn nanoparticles had higher antioxidant activity in comparison to $ZnSO_4$ (Salari et al. 2017). Yathisha et al. 2016 synthesised Zn nanoparticles using microwave assisted combustion. The microwaves applied in this method were allowed to penetrate into the material at molecular level thereby supplying energy throughout the material and producing Zn nanoparticles. Their method was found to be less time consuming for the production of nanoparticles and its major drawback is the consumption of high energy and low yield.

9.3.3 Green synthesis

Green synthesis is an emerging area in the field of bionanotechnology and provides economic and environmental benefits alternate to chemical and physical methods. In this method, non-toxic safe reagents which are eco-friendly and biosafe are used. Various natural resources available in nature such as plant extracts (Sithara et al. 2017), cyclodextrin (Abou-Okeil et al. 2012), chitosan (Mokhena and Luyt 2017) and many more have been studied for the synthesis of metal oxide nanoparticles. The use of plant extracts in the green synthesis of metal oxide nanoparticles has drawn a considerable attention as a straightforward approach (Nava et al. 2017; Sithara et al. 2017). Many researchers have reported the synthesis of metal oxide nanoparticles from plant extracts (Sithara et al. 2017; Jamdagni et al. 2016; Nava et al. 2017). Among those researchers, Nagarajan and Kuppusamy 2013 studied the extracellular synthesis of Zn nanoparticles from seaweed. The authors postulated that fucoidan water soluble pigment found in *Sargassum Myriocystum* can act as both reducing and stabilizing agents for the production of Zn nanoparticles. In addition to that, due to the availability of

Sargassum Myriocystum in all seasons the production of Zn nanoparticles can be easily scale up Nagarajan and Kuppusamy 2013. In other studies, Jamdagni et al. 2016 and Sithara et al. 2017 optimised the synthesis parameters of Zn nanoparticles and Ag nanoparticles, respectively. For instance, Sithara et al. 2017 optimised concentration of silver nitrate (a precursor), plant extract volume and temperature of the solution. From the results, the optimum concentration, volume and temperature were 1.75 mM, 0.5 mL and 50 °C, respectively. They also reported that the addition of plant extract to silver nitrate resulted in colour transformation from colourless to brown which confirms the formation of Ag nanoparticles (Sithara et al. 2017; Nakkala et al. 2017). To further confirm the formation of nanoparticles ultra violet visible (UV-vis) was used to measure the absorption of the spectrum at 300-500 nm. The band at 425 nm indicated the presence of Ag nanoparticles (Sithara et al. 2017).

9.3.4 Sol-gel technique

Sol-gel technique is a long established industrial process for producing colloidal nanoparticles from liquid phase and one of the most widely used and studied field of material chemistry (Danks et al. 2016; Charitidis et al. 2014). The origin of sol-gel chemistry was established in the 19^{th} century that an alkoxide prepared from silicon tetrachloride ($SiCl_4$) started to form a gel when exposed to air. This was later established to be driven by atmospheric moisture which caused hydrolysis of silicon alkoxide and then condensation (Danks et al. 2016). The sol-gel technique is generally considered as a chemical process used to prepare high purity inorganic-organic metal oxides in various forms such as aerogels, thin films, xerogels, fibres and micro/nanoparticles based on hydrolysis and condensation reactions as depicted in Figure 4.

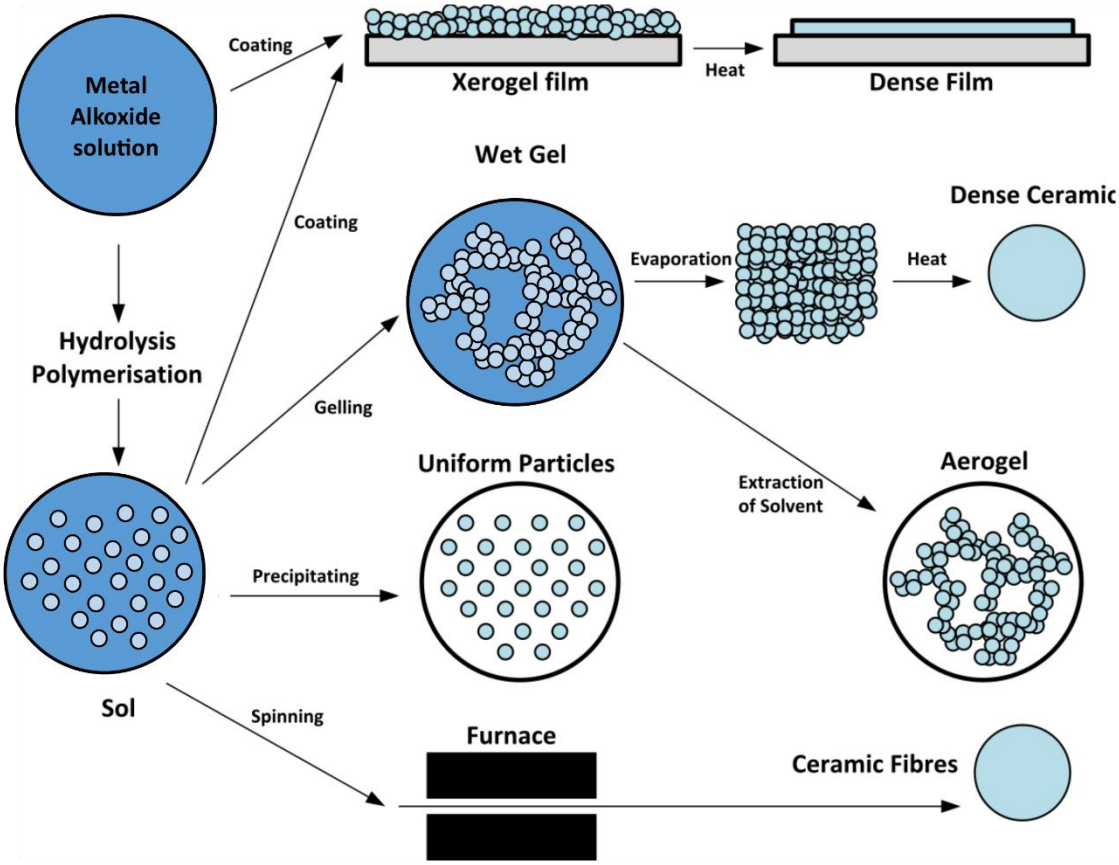

Figure 4 **Different stages and routes of the sol-gel technology. (Redrawn from https://en.wikipedia.org/wiki/Sol-gel)**

The fundamentals to mastering the sol-gel chemistry of alkoxide require understanding of the central hydrolysis and condensation reactions. The sol-gel chemistry is divided into two reaction steps; the first reaction step is hydrolysis, which produces hydroxyl groups, and the second reaction step is condensation, which involves the polycondensation of hydroxyl groups and residual alkoxyl groups to form a three-dimensional network. These steps are strongly influenced by process parameters such as the presence, type and concentration of catalyst, the ratio of water to alkoxide and in other cases the reaction of a metal chloride with either a metal alkoxide or organic ether acting as oxygen donors. Furthermore, the sol-gel process is divided into two preparation routes namely; hydrolytic route which involves water as a ligand and solvent (Niederberger 2009); non-hydrolytic route which involves ethers, alcohols and ketones as oxygen donors (Paderni et al. 2014). The sol-gel route offers various advantages such as low temperature conditions during processing, fine control of particle size and distribution, the choice of precursor, high yield and low production costs. Therefore this process is suitable for organic materials to be introduced into the system. On the other hand, in order to provide good reproducibility of the synthesis protocol, the sol-gel process has

large number of reaction parameters such as pH, temperature, hydrolysis and condensation rate of the metal oxide precursor, the nature and concentration of anions, method of mixing and mixing rate of oxidation that have to be strictly controlled. Owing to its advantages, the sol-gel technique has been widely used in the preparation of protective coatings (Landry et al. 2013), optical materials (Styskalik et al. 2017) and mesoporous materials (Lodha et al., 2012) because of their hardness, abrasion and scratch resistance, chemical and thermal stability with well-defined and controllable morphology and porosity. This led to more attraction of its application in the coating, biomedical, water filtration and sanitation industries.

9.3.4.1 Hydrolytic sol-gel (HSG) route

Hydrolytic sol–gel route is a chemical process used to synthesize various metal oxides (TiO_2, SiO_2, ZrO_2, Al_2O_3 and others) from a precursor based on hydrolysis and condensation reactions to form an integrated network of discrete particle in the presence of water at low temperature conditions. The method has been used to produce mesoporous materials, super-hydrophobic coating surfaces and fillers for polymers from a variety of alkylsilane precursors such as, tetraethyl orthosilicate or tetraethoxysilane (TEOS) (Morselli et al. 2013; Mokhothu et al. 2014b; Mokhothu et al. 2014a; Möller and Bein 2017; Colleoni et al. 2013), methyltrimethoxysilane (MTMS) (Xu et al. 2011), methyltriethoxysilane (METES) (Rao et al. 2011) and tetramethoxysilane (TMOS) (Alongi et al. 2012). The most widely used precursor in the hydrolytic sol-gel route is tetraethoxysilane (TEOS) to produce silica by hydrolysis and condensation reactions as indicated in Equations 1-3, in which hydrolysis of alkylsilane in acid or basic conditions, alcohol condensation and water condensation are presented.

$$\text{Si-}(OC_2H_5)_4 + 4H_2O \rightarrow \text{Si-}(OH)_4 + 4C_2H_5OH \quad (1)$$

$$\text{Si-}(OH)_4 + \text{Si-}(OC_2H_5) \rightarrow \equiv\text{Si-O-Si}\equiv + 4C_2H_5OH \quad (2)$$

$$\text{Si-(OH)} + \text{Si-(OH)} \rightarrow \equiv\text{Si-O-Si}\equiv + 4H_2O \quad (3)$$

According to the reactions, the alkylsilane initially hydrolyse in acid or basic conditions to form silicic acid which condensates with another alkylsilane or with itself to form a cross-linked polysiloxane network and then form a gel. The advantage of this process as depicted by the reaction equations is that modification or functionalization of the surface through organic groups such as silane coupling agents can be added to achieve desired properties.

Therefore the keystone in the development of adsorbents, coatings and mesoporous silica materials is through the introduction of reaction mixture with surfaces that can be selectively functionalized with multiple organic and inorganic groups.

For instance, porous, chemical and thermal stable mesoporous silica nanoparticles were prepared through hydrolytic sol-gel method using tetraethylorthosilicate (TEOS), methanol (CH_3OH), Cetyl Trimethylammonium Bromide (CTAB) and deionised water in the presence of sodium hydroxide as catalyst at 80°C temperature (Lodha et al., 2012). IT was reported that the mesoporous silica nanoparticles improved the solubility of poorly water soluble drugs and enhanced their absorption capacity. On the other hand, Möller and Bein 2017 investigated the functionality and structure of mesoporous silica nanoparticles by using various synthetic strategies to tune the pore size and pore topology of the mesoporous system for drug delivery applications. Mesoporous silica particles with an average particle size between 30 and 100 nm were achieved by varying the molar ratio between the silica precursor tetraethoxysilane (TEOS) and the catalyst polyalcohol triethanolamine (TEA). (Berendjchi et al. 2011) modified cotton fibre surface with silica particles prepared by sol-gel methods to produce superhydrophobic and antibacterial cotton surface. In this study, cotton fabric samples were impregnated with silica particles doped with two different amounts of copper (Cu) nanoparticles (0.5% and 2% wt/wt) and some samples were modified with hexadecyltrimethoxysilane (HDTMS). Cotton samples coated alkylsilane-treated SiO_2 were found to have higher surface roughness compared to the untreated cotton sample. The cotton samples were found to have a higher air trapping capability which resulted to high values of static water contact angle (SWC) (151.1°) and water shedding angle (30°). This was due to the interaction of a long-chain alkylsilane in HDTMS with silanol groups of silica thereby producing a hydrophobic surface. Furthermore, the addition of 0.5% (wt/wt) Cu into silica sol caused the silica nanoparticles to agglomerate in more grape-like clusters on the cotton fabrics and as a result increased the SWC (155° for a 10-µl droplet). All fabricated surfaces containing Cu nanoparticles displayed excellent antibacterial activity against both gram-negative and gram-positive bacteria. For reinforcing purpose, the hydrolytic route was used in the preparation of EPDM rubber reinforced with *in situ* generated silica particles (Mokhothu et al. 2014b; Morselli et al. 2013). In the case of Morselli et al. 2013 EPDM/SiO_2 composites were prepared in the absence of a coupling agent while (Mokhothu et al. 2014b) introduced bis-[-3-(triethoxysilyl)-propyl]-tetrasulfide (TESPT) as a coupling agent. From both studies, the incorporation of silica particles increased the thermal and mechanical properties of

EPDM. Nevertheless, EPDM/SiO_2 composites prepared in the presence of TESPT, the tensile results showed formation of longer crosslink chains in the presence of the coupling agent and gave rise to larger elongation at break values. This was attributed to the polysulfidic linkage from TESPT which produced strong reinforcement between the rubber and the filler, and gave rise to the larger stress at break values.

9.3.4.2 Non-hydrolytic sol-gel (NHSG) route

Non-hydrolytic sol-gel route is described as chemical process used to produce metal oxides with high crystallinity and purity in the absence of water compared to its hydrolytic counterpart. The NHSG process is divided into two steps. The first step involves the reaction of precursors (chlorides, alkoxides, and acetylacetonates) with oxygen donors (ethers, alcohols, ketones). The second step can follow different pathways depending on the alkoxide employed (Bilecka and Niederberger 2010; Hay and Raval 2001; Messori et al. 2009). The main non-hydrolytic routes involve the reaction of a metal chloride with either a metal alkoxide or organic ether, acting as oxygen donors as described from the below equations.

$$M\text{-}Cl_m + n\ R\text{-}OH \rightarrow M\text{-}(Cl)_{m-n}(OR)_n + n\ HCl \quad \text{(Step 1)}$$

$$\equiv M\text{-}OR + RO\text{-}M\equiv \rightarrow \equiv M\text{-}O\text{-}M\equiv + R\text{-}O\text{-}R \quad \text{(Step 2)}$$

$$\text{and/or } \equiv M\text{-}OR + Cl\text{-}M\equiv \rightarrow \equiv M\text{-}O\text{-}M\equiv + R\text{-}Cl$$

The advantage of the NHSG route over the HSG route is that reactions are usually slower and easier to control than HSG process and features different reactions and reaction conditions, which significantly affect the homogeneity, surface chemistry and texture of the resulting metal oxide (Bilecka and Niederberger 2010; Messori et al. 2009; Hay and Raval 2001). Furthermore, the NHSG route offers a wide variability in the choice of precursors and oxygen donors to allow control of the reaction rates resulting in homogeneous products with specific properties and compositions. In general terms, it is known that the non-hydrolytic route is potentially solvent-free, without difficulties with hydrophobic substances and particularly suitable for water-sensitive species (Hay and Raval 2001). Conversely, the formation of alkyl ethers and/or alkyl chloride as by-products and the potential incompatibility with oxygen-containing species have to be taken into account as possible negative aspects.

The possibility of preparing polymers reinforced with metal oxides generated in situ by a non-hydrolytic sol-gel process, has been investigated (Morselli et al. 2012a; Morselli et al. 2012b). The investigations focused on epoxy resin/titanium dioxide (TiO_2) and poly(methyl methacrylate) (PMMA)/titanium dioxide (TiO_2) nanocomposites. In both investigations titanium(IV)chloride ($TiCl_4$) was used as a precursor while benzyl alcohol (BzOH) as an oxygen donor. Both studies showed improvements in the mechanical properties, independent of the chosen polymer matrix. This was due to the improved interfacial interactions between the inorganic and organic phases brought about by the non-hydrolytic sol-gel route. Recently a review focusing on the synthesis, and application of various metal oxides produced by NHSG route has been reported (Styskalik et al. 2017). With emphasizes on the condensation reactions and deep insights into their mechanisms and applications of mixed oxides, silicates and phosphates. The application of NHSG derived materials as heterogeneous catalysts and supports, luminescent materials and electrode materials in Li-ion batteries are well documented.

9.4 Nanoclay minerals

Clay minerals are generally known as layered silicates or nanoclays because of their stacked structure of 1nm silicate sheets which are in nanoscale with a variable basal distance. Nanoclays are classified according to various main classes i.e. vermiculite, kaolirite, seipolite, bentonite, laponite, montmorillonite, attapulgite, halloysite and hectorite (Awad et al. 2004; Ali et al. 2016). Amongst them the most widely used layered silicate for reinforcing in polymer composites is montmorillonite (Azzam et al. 2013). Montmorillonite (MMT) is a 2 to 1 layered smectite clay mineral with a platy structure. Each layer is made up of two tetrahedral sheets having an octahedral sheet between them. Furthermore, the thickness of the individual platelet is around 1nm, but with surface dimensions from 300 to more than 600 nm, resulting in unusual high aspect ratio (Azzam et al. 2013). These layers are stacked and held together by van der Waals forces to form clay particles.

The increasing attention in using nanoclays (especially montmorillonites) as reinforcement in polymers is mainly due to their high cation exchange capacity (CEC), their high aspect ratio, their platelets' morphology, the degree to which the clay can absorb and exchange cations, their large surface area, as well as their natural abundance and low cost. Because of their inherent properties, clay minerals have found a wide range of applications which are widely

studied by many disciplines and reported in literature (Ali et al. 2016; Kleyi et al. 2016; Hernández-Hernández et al. 2016). Reinforcing of polymer matrices with clay minerals promote important technical advantages such as improvement in (i) flame resistance, (ii) rheological properties, (iii) mechanical properties, (iv) thermal properties, and (v) barrier properties. Polymer-clay nanocomposites (PCN) can be prepared from three main fabrication methods according to the processing techniques and starting materials. The methods are solution mixing, *in situ* polymerization and melt mixing; they are methods utilized to produce better PCN where the morphology of the clay layers can be controlled. Hence, the performance and properties of polymer-clay nanocomposites is influenced by the interaction and dispersion of silicate layers in the polymer matrix. Depending on the interaction between the clay and the polymer matrix the achievable dispersions can be (i) polymer chains can intercalate in between the clay galleries, (ii) silicate layers can exfoliate in the polymer and (iii) phase separated where there's no interaction between the polymer and clay layers and therefore no separation of clay layers as shown in Figure 5. Another important aspect in polymer-clay nanocomposites is the characterization of the nanocomposites to study the degree of dispersion of clay layers which affects the final properties of the nanocomposites. Several techniques have been used to study the nanostructure of PCNs and clay, and they include transmission electron microscopy (TEM), neutron scattering methods, X-ray diffraction (XRD) and neutron magnetic resonance (NMR) spectroscopy. However, TEM and XRD are the most commonly used techniques and Figure 5 shows the relation between different states of dispersion of nanoclays in a polymer matrix.

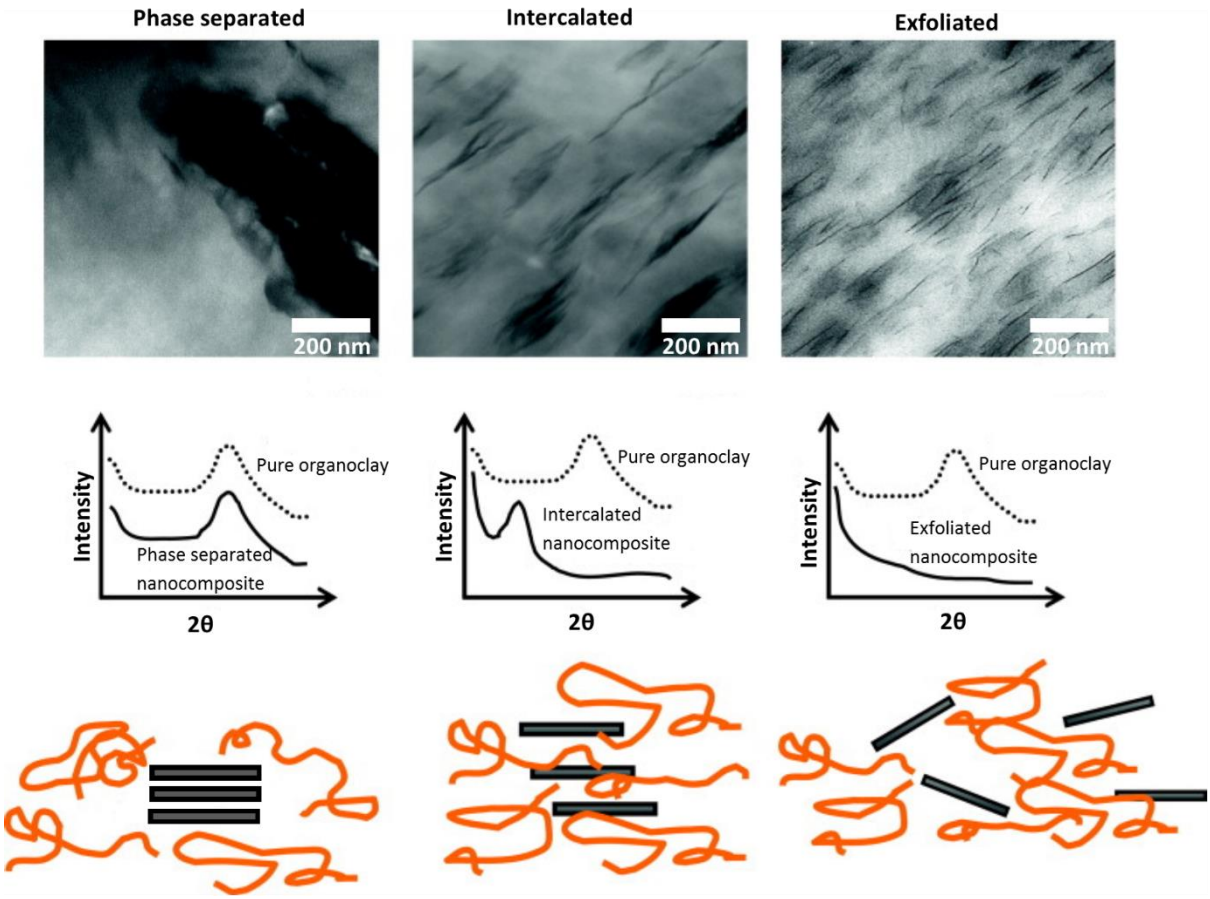

Figure 5 **Various organoclay dispersion state in polymer matrix observed through TEM and XRD analysis. Redrawn from (Paul and Robeson 2008), with permission from Elsevier.**

9.4.1 Solution mixing technique

The solution mixing technique involves the exfoliation of clay layers into single layers using a solvent in which the polymer or prepolymer is soluble (Hernández-Hernández et al. 2016). Clay layers are firstly swollen or dispersed in the solvent followed by the addition of the dissolved polymer into the clay solution. The solvent allows polymer chains to be embedded into the exfoliated clay layers and afterwards the solvent is evaporated, the polymer chains merge with the dispersed clay layers as depicted in Figure 6.

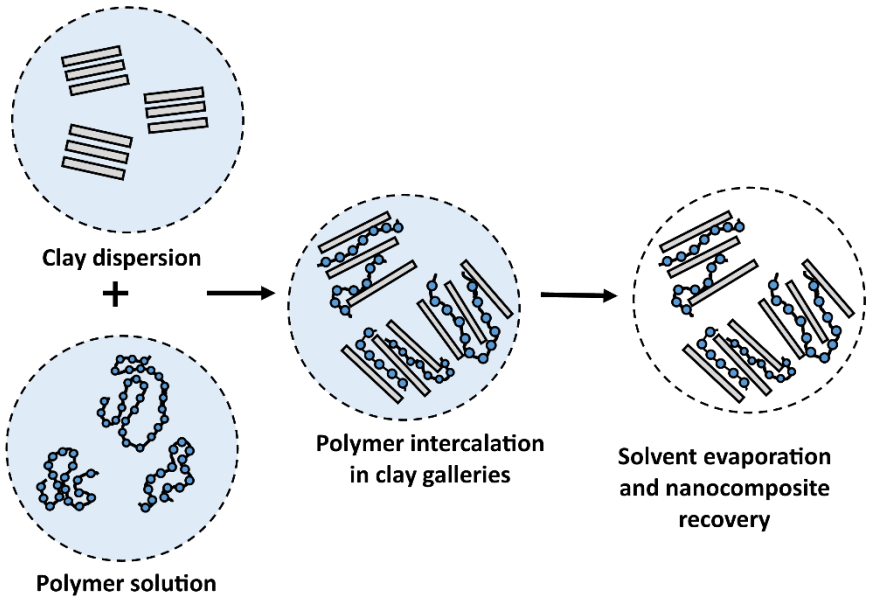

Figure 6 **Solution mixing of polymer clay nanocomposites. Redrawn from (Hernández-Hernández et al. 2016) Open Access**

The advantage of solution mixing is the low viscosity of the solution that allows particle dispersion (Silva et al. 2014). Several studies have used this technique to achieve high degree of interaction and dispersion between the layered silicates and polymer matrices. For instance, water soluble polymers reinforced montmorillonite nanocomposite were prepared using solution mixing methods; (Billingham et al. 1997) investigated the adsorption of polyethylene glycol (PEG), poly(acrylic acid) and polyamine onto a clay mineral surface while (Strawhecker and Manias 2000), used polyvinyl alcohol (PVA) and poly(ethylene oxide) (PEO) by (Malwitz et al. 2003). Their results showed that water soluble polymers were able to adsorb onto clay dispersions and were stable when deposited as thin solid films. This was believed to be caused by the polarity of the polymers which enabled intercalation. In another study, modified montmorillonites (O-MMTs, denoted 15A, 20A and 30B) were used to prepare polypropylene (PP)-based composites (Chiu and Chu 2006). They reported that TEM and XRD results showed intercalation and exfoliation of the polymer in the three O-MMTs in PP matrix which indicating the successful formations of PP/O-MMT nanocomposites. Furthermore, TGA results confirmed the enhanced thermal stability of PP after the addition the modified montmorillonites. This indicated that the nanoclays were homogeneously disperse in the nanocomposites prepared by solution intercalation and acted as a barrier for energy transport as reported by (Silva et al. 2014), in the preparation of high density polyethylene/clay and carbon nanotube nanocomposites *via* solution and melting

intercalation methods. Furthermore, it was also observed that both preparation methods improved the mechanical properties of PP by increased both the hardness and modulus.

9.4.2 In situ polymerization technique

In this method, polymer clay nanocomposites are prepared from a monomer solution or liquid monomer in which the clay layers are swelled such that polymerization of the polymer occurs in between the clay layers (Figure 7). The *in situ* polymerization process can be carried out by means of radiation, organic initiator or heat. The polymer has the ability to grow in between the clay layers thereby pushing them apart and as result lead to intercalated or exfoliated dispersion. However, the *in situ* polymerization process is limited due to lack of suitable monomers and compatible solvents ((Hernández-Hernández et al. 2016).

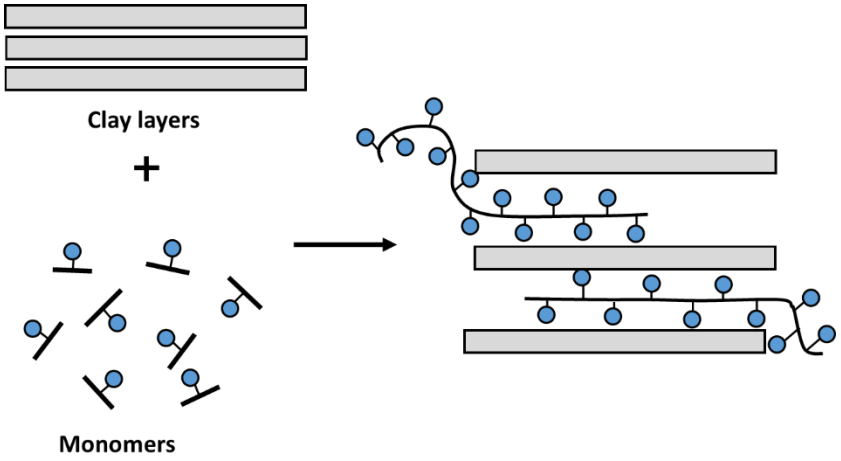

Figure 7 ***In situ*** **polymerization of polymer clay nanocomposites. Redrawn from (Hernández-Hernández et al. 2016). Open Access**

9.4.3 Melt mixing technique

The melt mixing technique the most popular method in industry which is environmentally viable and economically attractive because it does not require the use of organic solvents and preparation of nanocomposites can be produced using scalable compounding techniques such as melt extrusion and injection moulding. Melt mixing is a process whereby layered silicates are mixed with thermoplastic polymers in their molten state. The applied shear allows destruction of clay layers and as a result the molten polymer chains are able to stack in between the clay layers to form intercalated structure (Figure 8).

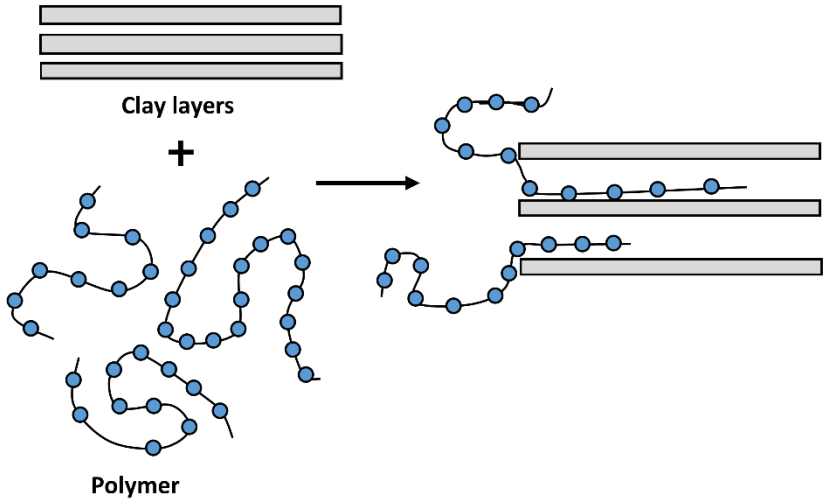

Figure 8 **Melt mixing of polymer clay nanocomposites Redrawn from (Hernández-Hernández et al. 2016). Open Access**

However, some disadvantages associated with the melt mixing technique is the formation of aggregates at high clay loading leading to micro-composites rather than nanocomposites. Again the technique uses hydrophobic polymer matrices that are not compatible with layered silicates leading to poor dispersion and interaction between the two components. Interestingly, researchers have found ways to overcome these setbacks by introducing chemical modification on layered silicates (Bandyopadhyay et al. 2010; Bandyopadhyay et al. 2017), introduction of maleic anhydride modified polymers to enhance compatibility (Liang et al. 2004), and the use of organosilane coupling agents to improve interaction between the clay layers and the polymer (Sibeko and Luyt 2014; Sibeko and Luyt 2013).

9.5 Nanocellulose

Nanocellulose are classified into cellulose nanocrystal (CNC) and cellulose nanofibres (CNF). Both CNC and CNF are extracted from purified cellulose obtained from various lignocellulosic fibres and bacteria cellulose. CNC are rod-like shaped containing only crystalline domain. CNF on the other hand are web-shaped fibres stabilized by hydrogen bonds and they consist of both crystalline and amorphous domains. However, the isolation approaches of these materials are different. For example, CNC can be isolated by acid and enzymatic hydrolysis whereas CNF can be isolated by mechanical, chemo-mechanical and the combination of enzyme and mechanical process. Since the introduction of

bionanotechnology, the interest has been diverted towards the isolation and characterization of nanocellulose. The reason for this could be explained by the fact that nanocellulose has shown impressive properties. These properties include high aspect ratio, large surface area, high crystallinity, transparency, and high mechanical properties which make them suitable for composite materials (Jonoobi et al. 2015). In addition to this, nanocellulose are regarded as the new generation of biobased reinforcement for the development of high performance composite materials due to their extraordinary properties.

9.5.1 Isolation and characterization of CNC

As stated previously, CNC are isolated by acid and enzyme hydrolysis of cellulose fibres obtained from lignocellulose fibres. Different acids as well as the mixture of acids have been investigated (Kasiri and Fathi 2017; Li et al. 2015; Alves et al. 2015; Mtibe et al. 2015). Sulphuric acid is widely used for the extraction of CNC (Mtibe et al. 2015; Mokhena and Luyt 2014). The extraction process of rod-like shaped CNC involves the removal of amorphous regions from cellulose fibres by strong acid and thus producing high pure CNC. To terminate the acid hydrolysis treatment, the suspension containing CNC may either be diluted by adding 10 folds of water or ice cubes. Afterwards, the diluted suspension undergoes centrifugation followed by dialysis to remove excess acid. Finally, CNC is then subjected to ultra-sonication for dispersion and subsequently adding few drops of chloroform to prevent fungal growth (Mtibe et al. 2015). Depending on their applications and characterization, CNC may either be stored in the refrigerator or freeze dried. For example, in-situ polymerization requires both dried and CNC suspension (Mtibe et al. 2015). The properties of CNC depends on the source of cellulose fibres, pre-treatment methods and experimental conditions (Kargarzadeh et al. 2012). The diameters of CNC are in nano-scale and lengths in micro-scale (Kargarzadeh et al. 2012; Motaung and Mtibe 2015; Mokhena and Luyt 2014). An example of CNC is depicted in Figure 9.

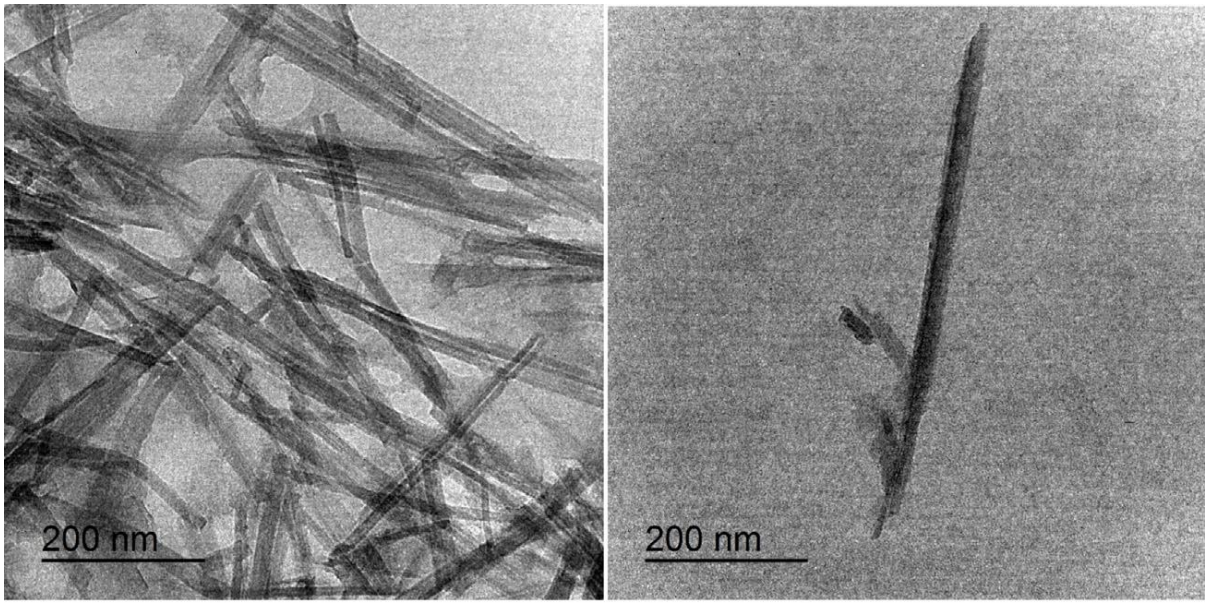

Figure 9 TEM image of CNC extracted from seaweed (Singh et al. 2017).

The morphology of CNC are usually studied by TEM, AFM and polarized light scattering (Mtibe et al. 2015; Mokhena and Luyt 2014). For instance, Mtibe et al. 2015 extracted CNC from cellulose obtained from maize stalk residues with dimeters ranging from 3 to 7 nm and the lengths were ranging from 150 to 450 nm. The dimensions of CNC were measured by AFM microscopy. In addition, CNC showed a flow of birefringence which is an indication of isolated nanocrystals and good dispersion. Mokhena and Luyt 2014 measured the dimensions of CNC extracted from sisal fibres by TEM. They reported that the obtained CNC had an average diameters of 12.2 ± 3.7 nm, average lengths of 197 ± 75 nm and aspect ratio of 16. As mentioned previous that acid hydrolysis removes amorphous regions of the fibres leaving crystalline region. Li et al. 2009 investigated the crystallinity of CNC using XRD. From their results, they reported that crystallinity increased for CNC when compared to cellulose due to the realignment of crystals which leads to the increase in crystallinity. These authors also investigated thermal stabilities of CNC using thermogravimetric analysis (TGA). From their results, CNC displayed two degradation steps which correspond to decomposition of more accessible regions to acid (highly sulphated region) and decomposition of unsulphated region, respectively. These results were in agreement with the results reported by other authors (Kargarzadeh et al. 2012; Silvério et al. 2013; Flauzino Neto et al. 2013). Acid hydrolysis suffers several drawbacks such as low yield and the use of strong acids which are not eco-friendly. However, Mathew et al. 2014 proposed a process of scaling up the production of CNC using a user friendly method. In their study, the gel-like CNC was produced by passing

2 litres of cellulose through high pressure homogenizer at a pressure of 500 bars. For comparison, CNC were extracted by sulphuric acid using lab scale process. The yield of CNC using pilot scale production process was found to be 100% with respect to the extracted cellulose which was higher when compared to that of the lab scale process.

Another eco-friendly method for preparing CNC is enzyme hydrolysis (Teixeira et al. 2015). The principle of this method is similar to that of acid hydrolysis treatment whereas enzymes break glyosidic bonds of amorphous domain thereby producing individual highly crystalline particles. The major drawback of enzyme hydrolysis is that it produces less stable CNC when compared to that of acid hydrolysis (Satyamurthy et al. 2011).

9.5.2 Isolation and characterization of CNF

CNF are extracted from the cell wall of lignocellulose fibres by various methods. These methods include mechanical, chemo-mechanical and enzymatic combined with mechanical process (Jonoobi et al. 2015). Unlike CNC, CNF contains both crystalline and amorphous regions (Jonoobi et al. 2015). The defibrillation of cellulosic fibre into individual CNF requires an extensive mechanical grinding (Lekha et al. 2016). However, the pre-treatment of fibres is required to facilitate the defibrillation process. The micrograms of CNF obtained using various disintegrating technique are shown in Figure 10.

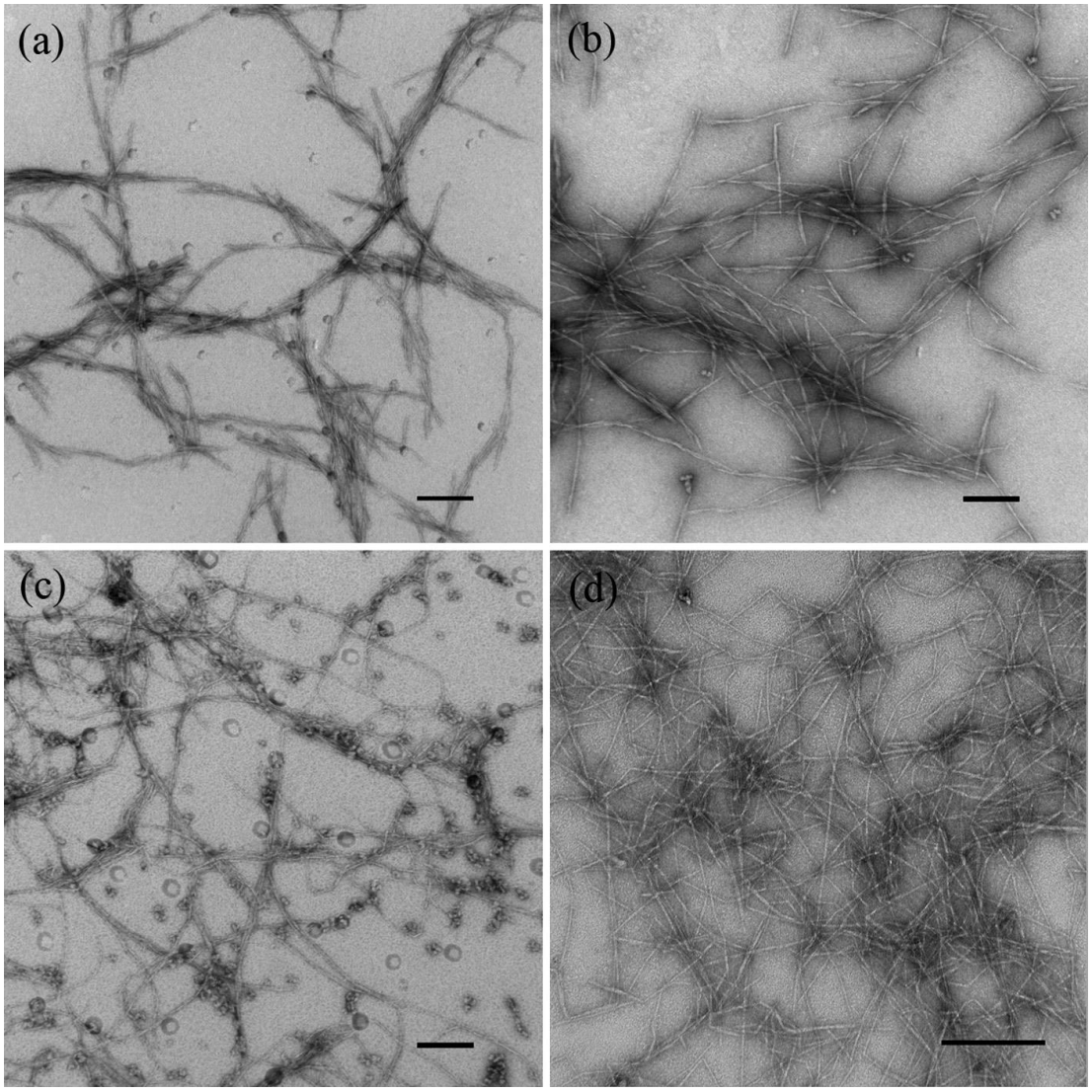

Figure 10 (a) CNF extracted by enzyme and mechanical grinding, (b) CNF extracted by enzyme and the combination of mechanical grinding and microfluidization, (c) CNF extracted by a combination of mechanical grinding and microfluidization and (d) CNF extracted by 2,2,6,6-tetramethylpiperidinyl-1-oxyl (TEMPO) oxidation and microfluidization. The scale bar is 200 nm (Qing et al. 2013).

The pre-treatment is usually performed using chemicals or enzymes prior mechanical process in order to attain superior properties of CNF as well as to reduce energy consumption (Jonoobi et al. 2015). 2,2,6,6-tetramethylpiperidinyl-1-oxyl (TEMPO) oxidation is one of the common pre-treatment of fibres. Fujisawa et al. 2011 pre-treated wood fibre by TEMPO oxidation followed by disintegration in homogenization at 15000 rpm for 5 or 10 min and subsequently sonicated for 2, 4 or 20 min in order to produce longer CNF. From the results, TEM revealed that uniform CNF with width of 4 nm and lengths in few microns were

extracted. The authors claimed that the yield of CNF produced after 10 min in a homogenizer and sonicated for 10 min was approximately 100% and 85 % for CNF produced after 5 minutes in a homogenizer and sonicated for 2 minutes. In addition, CNF were used to produce flexible transparent films after drying. Qing et al. 2013 produce CNF using mechanical grinding and microfluidization combined with TEMPO oxidation and enzymatic pre-treatment. During mechanical grinding, dilute slurry is passed between two grinding stones (one is stagnant and the other rotates). The surface of the stones has grooves of which the slurry is exposed to cyclic stresses (Yousefi et al. 2013). The refined slurry from mechanical grinding was further refined through microfluidization by passing it 15 times at a pressure of 150 MPa. The extracted CNF were used to develop thin films also called nanopapers. From TEM results, the authors reported that the combination of mechanical grinding and microfluidization resulted in finer fibres of diameters ranges from 4.7 to 31 nm. In the case of enzyme pre-treatment, it was observed that the enzymes reduced the length of fibres which produced short rod-like shaped fibres with diameters range from 16-87 nm. Furthermore, CNF produced from TEMPO oxidation and microfluidization were uniform with narrow diameters range of 5–7 nm. Interestingly, both mechanical grinding and microfluidization randomly breaks apart both crystalline and amorphous regions which leads to the decrease in crystallinity of CNF. This breakage of cellulose fibre crystals is believed to separate the bundles of fibrils to form nanofibres. The reduction of crystallinity after mechanical process were also confirmed by Mtibe et al. 2015 and Yousefi et al. 2013. In addition, Yousefi and co-workers 2013 also investigated the thermal stabilities of thin films prepared from CNF. They reported that CNF films prepared from canola strew showed lower thermal stability in comparison to micropaper prepared from bacteria cellulose and bacteria cellulose CNF. The authors suggested that the reason for the decrease in thermal stabilities was because of lower crystallinity.

Most recently, Jonoobi et al. 2012 estimated the cost and the yield of CNF obtained from sludge in order to benefits the usage of sludge (bioresidue) as a raw material. The yield of CNF was found to be 95%. The estimation of costs was based on the material cost and the energy consumption during defibrillation. The sludge was obtained at no cost. However, the energy cost per megawatt per hour was approximately $113 per ton and the total cost was approximately $113 per ton. Therefore, the authors indicated that this method can be easily scalable and is it economical and commercially feasible. Another advantage of mechanical grinding it does not require the use of chemicals which are not environmental benign.

9.6 Summary

In this chapter fabrication methods of various nanomaterials and their characterization as well as challenges involved during their preparation were presented. From the above discussions, it is clear that the application of nanomaterials from nanocellulose, metal oxide, carbonaceous materials and clay minerals have received significant attention globally particularly due to their inherent properties such particle size, larger surface area, compositions, crystallinity, shape and many more. These features of nanomaterials are characterized by various characterization techniques such as SEM, TEM, AFM, BET, EDX, TGA and XRD. The characteristics of nanomaterials are very vital to determine their applications in various fields of material science and industrial application. Various methods were discussed focusing on the development of innovative technologies for engineering nanomaterials and possible industrial scale.

Highly crystalline cellulose nanocrystals (CNC) obtained from different lignocellulosic fibres were produced from acid and enzyme hydrolysis techniques. Both acid and enzyme hydrolysis remove amorphous regions to produce highly crystalline CNC. CNC with diameters ranging from 3-12.2 nm and an average length of 150-450 nm were produced but, drawbacks such as low yield and use of strong acids limit their applications for industrial upscaling. On the other hand, a pilot scale high pressure homogenizer was observed to produce high yield (100%) of CNC compared to acid and enzyme hydrolysis. Moreover, another environmentally friendly and cost effective technique reported was the mechanical grinding method which was used to produce cellulose nano-fibres (CNF). This technique was reported to be easily scalable and commercially feasible and can be coupled with micro-fluidization to produce CNF with diameters ranging from 4-31 nm or in combination with enzyme pre-treatment to produce short rod-like CNF with diameters ranging from 16-87nm. Though this technique is feasible it should be noted that this technique offers CNF with low crystallinity due to high mechanical grinding on fibres when producing nanofibers.

In the synthesis of metal oxides, different preparation methods such as chemical synthesis, combination of physical and chemical, green synthesis and sol-gel route were used to produce various metal oxides suitable for photocatalytic, coatings, adsorbents and drug deliver applications. Synthesis of metal oxide is mainly depended on the type of precursor as well as the processing conditions which play a vital role in the final product and its application.

However, the use of toxic and costly chemicals, production of secondary waste, consumption of high energy and low yield are major drawbacks of chemical synthesis and combination of physical and chemical synthesis, respectively. On the other hand, green synthesis of Zn and Ag nanoparticles from plant extracts was reported as possible technique for upscaling due to the availability of seaweed species (*Sargassum Myriocystum*) throughout the seasons. Another engineering technique that has drawn attention in the synthesis of various metal oxides for vast application is the sol-gel route and one of the mostly used industrial processes. Various forms of products such as aerogels, thin films, micro/nanoparticles, mesoporous material, xerogels and fibres have been produced from this technique and have drawn attraction in biomedical, coatings and water filtration applications.

In the preparation of nanoclays, melt mixing technique is the most popular methods for industrials application as compared to its counterpart solution mixing and *in situ* polymerization techniques. The melt mixing method is environmental viability and preparation of nanocomposites can be produced using scalable compounding techniques such as melt extrusion and injection moulding.

Carbonaceous nanomaterials are the most fascinating materials because of their large surface area, high thermal stability, electrical conductivity and high mechanical properties. Carbon nanotubes and graphite nano-sheets possess extensive potential in various application due to their unique properties and their fabrication plays a vital role in the production of electrical and thermal conductivity materials and as filler in polymeric matrices. Electric arc-discharge and laser ablation are one of the methods used to fabricate multiwall and single wall nanotubes, however due to setbacks such as high energy consumption and low yields unfortunately these methods are not economically viable for industrial upscaling. Nonetheless, chemical vapour deposition (CVD) is regarded as suitable technique for production of high quality and well orientated CNTs at a large scale production. Again, CVD is economically viable because the process is easy to operate, can produce vertically and horizontally aligned CNTs and availability of raw material in the form of hydrocarbon gases and plastic waste. In the production of exfoliated graphite nano-sheets, mechanical and thermal exfoliation of graphite oxide and/or graphite is established as the two major techniques. This is because exfoliation of bulk graphite material is of great importance, as many applications rely on large scale production of exfoliated materials with controlled properties. In addition, extensive effort has been made to improve the yield and degree of

exfoliation, but the yield of monolayer graphene is still quite low. Hence, in many cases centrifugation is employed to remove unexfoliated graphite. Nevertheless, exfoliation methods with higher yields are still of critical interest.

References

Abou-Okeil, A., Amr, A., and Abdel-Mohdy, F. A. 2012. Investigation of Silver Nanoparticles Synthesis Using Aminated β-Cyclodextrin. *Carbohydrate Polymers* 89, 1–6.

Ali, F., Ullah, H., Ali, Z., Rahim, F., Khan, F., and Rehman, Z. U. 2016. Polymer-clay nanocomposites, preparations and current applications : A review. *Current Nanomaterials* 1, 1–13.

Allen, M. Tung, V. C., and Kaner, R. B. 2009. Honeycomb carbon: A study of graphene. *American Chemical Society* 110, 132–145.

Almkhelfe, H., Li, X., Rao, R., and Amama, P. B. 2017. Catalytic CVD Growth of Millimeter-Tall Single-Wall Carbon Nanotube Carpets Using Industrial Gaseous Waste as a Feedstock. *Carbon* 116 181–90.

Alongi, J., Ciobanu, M., and Malucelli, G. 2012. Thermal Stability, Flame Retardancy and Mechanical Properties of Cotton Fabrics Treated with Inorganic Coatings Synthesized through Sol-Gel Processes. *Carbohydrate Polymers* 87, 2093–99.

Alves, M., Neto, W. P. F. Alves, H., Ferreira, D., Vinícius, L., Gurgel, A., Barud, A., Carlos, S., Morais, L., and Daniel, P.. 2015. Kinetic Study of the Thermal decomposition of cellulose nanocrystals with different polymorph, cellulose I and II, extracted from different sources and using different types of acids. *Industrial Crops & Products* 76, 128–40.

Awad, W. H., Gilman, J. W., Nyden, M., Harris, R. H., Sutto, T. E., Callahan, J., Trulove, P. C., DeLong, H, C., and Fox, D. M. 2004. Thermal Degradation Studies of Alkyl-Imidazolium Salts and Their Application in Nanocomposites. *Thermochimica Acta* 409 3–11.

Azzam, E. M.S., Sayyah, S. M., and Taha, A. S.2013. Fabrication and characterization of nanoclay composites using synthesized polymeric thiol surfactants assembled on gold

nanoparticles. *Egyptian Journal of Petroleum* 22 493–99.

Bajad, G. S., Vijayakumar, R.P., Gupta, A. G., Jagtap, V., and Singh, Y.2017. Production of liquid hydrocarbons, carbon nanotubes and hydrogen rich gases from waste plastic in a multi-core reactor. *Journal of Analytical and Applied Pyrolysis* 125 83–90.

Bandyopadhyay, J., Ray, S. S., and Bousmina, M. 2010. Effect of nanoclay incorporation on the thermal properties of poly(ethylene terephthalate)/liquid crystal polymer blends. *Macromolecular Materials and Engineering* 295 822–37.

Bandyopadhyay, J., Ray, S. S., Ojijo, V., and Khoza, M. 2017. Development of a highly nucleated and dimensionally stable isotactic polypropylene/nanoclay composite using reactive blending. *Polymer* 117 37–47.

Ben B., Abir, Hinkov, I., Yahia, S. B., Brinza, O., and Farhat, S. 2016. Arc discharge boron nitrogen doping of carbon nanotubes. *Materials Today Communications* 8. 183–95.

Berendjchi, A., Khajavi, R., and Yazdanshenas, M. E. 2011. Fabrication of superhydrophobic and antibacterial surface on cotton fabric by doped silica-based sols with nanoparticles of copper. *Nanoscale Research Letters* 6 594–602.

Berkmans, J. A., Jagannatham, M., Reddy, D. R., and Haridoss, P. 2015. Synthesis of thin bundled single walled carbon nanotubes and nanohorn hybrids by arc discharge technique in open air atmosphere. *Diamond and Related Materials* 55 12–15.

Bijanzad, K., Tadjarodi, A., and Akhavan, O. 2015. Photocatalytic activity of mesoporous microbricks of ZnO nanoparticles prepared by the thermal decomposition of bis(2-aminonicotinato) zinc (II). *Chinese Journal of Catalysis* 36 742–749.

Bilecka, I., and Niederberger, M. 2010. New developments in the nonaqueous and/or non-hydrolytic sol-gel synthesis of inorganic nanoparticles. *Electrochimica Acta* 55 7717–7725.

Billingham, J., Breen, C., and Yarwood, J. 1997. Adsorption of polyamine, polyacrylic acid and polyethylene glycol on montmorillonite: An in situ study using ATR-FTIR. *Vibrational Spectroscopy* 14 19–34.

Bonaccorso, F., Lombardo, A., Hasan, T., Sun, Z., Colombo, L., and Ferrar,. A. C. 2012. Production, processing and placement of graphene and two dimensional crystals. 1–28.

http://arxiv.org/abs/1212.3319.pdf.

Bota, P. M., Dorobantu, D., Boerasu, I., Bojin, D., and Enachescu, M. 2017. New laser ablation chamber for producing carbon nanomaterials using excimer laser. *Materials Research Innovations* 19 33–39.

Cai, M., Thorpe, D., Adamson, D. H., and Schniepp, H. C. 2012. Methods of graphite exfoliation. *Journal of Materials Chemistry* 22 24992–25002.

Charitidis, C. A., Georgiou, P., Koklioti, M. A., Trompeta, A. F., and Markakis, V. 2014. Manufacturing nanomaterials: From research to industry." *Manufacturing Review* 1: 1–19.

Chernysheva, M., Rozhin, A., Fedotov, Y., Mou, C., Arif, R., Kobtsev, S. M. Dianov, E. M., and Turitsyn, S. K. 2017. Carbon nanotubes for ultrafast fibre lasers. *Nanophotonics* 6 1–30.

Chiu, F. C., and Chu, P. H. 2006. Characterization of solution-mixed polypropylene/clay nanocomposites without compatibilizers. *Journal of Polymer Research* 13 73–78.

Choi, S. B. Byeon, C. C. Park, D. J., and Jeong, M. S. 2016. Polarization-selective alignment of a carbon nanotube film by using femtosecond laser ablation. *Journal of the Korean Physical Society* 68, 201–214.

Chrzanowska, J., Hoffman, J., Małolepszy, A., Mazurkiewicz, M., Kowalewski, T. A., Szymanski, Z., and Stobinski, L. 2015. "Synthesis of carbon nanotubes by the laser ablation method: Effect of laser wavelength. *Physica Status Solidi (B)* 252 1860–1867. doi:10.1002/pssb.201451614.

Colleoni, C., Donelli, I., Freddi, G., Guido, E., Migani, V., and Rosace, G. 2013. A novel sol-gel multi-layer approach for cotton fabric finishing by tetraethoxysilane precursor. *Surface and Coatings Technology* 235. 192–203.

Cooper, A. J., Wilson, N. R. Kinloch, I. A. and W Dryfe, R. A. 2014. Single stage electrochemical exfoliation method for the production of few-layer graphene via intercalation of tetraalkylammonium cations. *Carbon* 66 340–350.

Danks, A. E., Hall, S. R., and Schnepp, Z. 2016. The evolution of 'sol–gel' chemistry as a technique for materials synthesis. *Materials Horizons* 3 91–112.

Dunens, O.M., MacKenzie, K. J., and Harris, A. T. 2010. Large-scale synthesis of double-walled carbon nanotubes in fluidized beds. *Industrial & Engineering Chemistry Research* 49 4031–4035.

Eatemadi, A., Daraee, H., Karimkhanloo, H., Kouhi, M., Zarghami, N., Akbarzadeh, A., Abasi, N., Hanifehpour, Y., and Joo, S. W. 2014. Carbon nanotubes: properties, synthesis, purification, and medical applications. *Nanoscale Research Letters* 9 1–13.

Elumalai, K., and Velmurugan, S. 2015. Green synthesis, characterization and antimicrobial activities ofzinc oxide nanoparticles from the leaf extract of azadirachta indica (L.). *Applied Surface Science* 345 329–36.

Fang, X., Shashurin, A., Teel, G., and Keidar, M. 2016. Determining synthesis region of the single wall carbon nanotubes in arc plasma volume. *Carbon* 107 273–80.

Fujisawa, S., Okita, Y., Fukuzumi, H., Saito, T., and Isogai, A. 2011. Preparation and characterization of TEMPO-Oxidized cellulose nanofibril films with free carboxyl groups. *Carbohydrate Polymers* 84 579–83.

Gómez-Navarro, C., Weitz, R. T., Bittner, A. M., Scolari, M., Mews, A., Burghard, M., and Kern K. 2007. Electronic transport properties of individual chemically reduced graphene oxide sheets. *Nano Letters* 7 3499–3503.

Goyal, G., Hwang, J., Aviral, J., Seo, Y., Jo, Y., Son, J., and Choi, J. 2017. Green synthesis of silver nanoparticles using β-glucan, and their incorporation into doxorubicin-loaded water-in-oil nanoemulsions for antitumor and antibacterial applications. *Journal of Industrial and Engineering Chemistry* 47 179–186.

Greco, A., Timo, A., and Maffezzoli, A. 2012. Development and characterization of amorphous thermoplastic matrix graphene nanocomposites. *Materials* 5 1972–1985.

Hay, J. N., and Raval, H. M. 2001. Synthesis of organic-inorganic hybrids via the non-hydrolytic sol-gel process. *Chemistry of Materials* 13 3396–3403.

Hernández- Hernández, K. A., Illescas, J., Díaz-Nava, M. C., Muro-Urista, C. R., Martínez-Gallegos, S., and Ortega-Aguilar, R. E. 2016. Polymer-clay nanocomposites and composites: structures, characteristics, and their applications in the removal of organic compounds of environmental interest. *Medicinal Chemistry* 6 201–210.

Hong, Y., Wang, Z., and Jin, X. 2013. Sulfuric acid intercalated graphite oxide for graphene preparation. *Scientific Reports* 3 1–6.

Hou, B., Wu, C., Inoue, T., Chiashi, S., Xiang, R., and Maruyama, S. 2017. Extended alcohol catalytic chemical vapor deposition for efficient growth of single-walled carbon nanotubes thinner than (6,5). *Carbon* 119 502–10.

Hummers, W. S., and Offeman, R. E. 1958. Preparation of graphitic oxide. *Journal of the American Chemical Society* 80 1339. doi:10.1021/ja01539a017.

Iijima, S.. 1991. Helical microtubules of graphitic carbon. *Nature*. 354 1–2. doi:10.1038/354056a0.

Ionescu, M. I., Zhang, Y., Li, R., Sun, X., Abou-Rachid, H., and Lussier, L. S. 2011. Hydrogen-free spray pyrolysis chemical vapor deposition method for the carbon nanotube growth: Parametric studies. *Applied Surface Science* 257 6843–6849.

Jamdagni, P., Khatri, P., and Rana, J. S. 2016. Green synthesis of zinc oxide nanoparticles using flower extract of nyctanthes arbor-tristis and their antifungal activity. *Journal of King Saud University - Science*. http://dx.doi.org/10.1016/j.jksus.2016.10.002

Jayasena, B., and Subbiah, S. 2011. A novel mechanical cleavage method for synthesizing few-layer graphenes. *Nanoscale Research Letters* 6 1–7.

Ji, X., Zhang, W., Li, X., Yu, H., and Dong, H. 2017. A novel hybrid method combining ASP with PECVD for in- situ low temperature synthesis of vertically aligned carbon nanotube films. *Diamond and Related Materials* 77 16–24.

Jia, X., and Wei, F. 2017. Advances in production and applications of carbon nanotubes. *Topics in Current Chemistry* 375 1–35.

Jonoobi, M., Mathew, A. P., and Oksman, K. 2012. Producing low-cost cellulose nanofiber from sludge as new source of raw materials. *Industrial Crops and Products* 40 232–238.

Jonoobi, M. Oladi, R., Davoudpour, Y., Oksman, K., Dufresne, A., Hamzeh, Y., and Davoodi, R. 2015. Different preparation methods and properties of nanostructured cellulose from various natural resources and residues: A review. *Cellulose* 22 (2): 935–969.

Kamel, S. 2007. Nanotechnology and its applications in lignocellulosic aomposites, a mini review. *Express Polymer Letters* 1 546–75.

Kargarzadeh, H., Ahmad, I., Abdullah, I., Dufresne, A., Zainudin, S. Y., and Sheltami. R. M. 2012. Effects of hydrolysis conditions on the morphology, crystallinity, and thermal stability of cellulose nanocrystals extracted from kenaf bast fibers. *Cellulose* 19 855–866.

Kasiri, N., and Fathi, M. 2017. Production of cellulose nanocrystals from pistachio shells and their application for stabilizing pickering emulsions. *International Journal of Biological Macromolecules*. , http://dx.doi.org/10.1016/j.ijbiomac.2017.08.112

Kim, H. H., and Kim, H. J. 2006. Preparation of carbon nanotubes by DC Arc discharge process under reduced pressure in an air atmosphere. *Materials Science and Engineering: B* 133 (1–3): 241–44.

Kleyi, P. E., Ray, S. S., Abia, A. L. K., Ubomba-Jaswa, E., Wesley-Smith, J., and Maity, A. 2016. Preparation and evaluation of quaternary imidazolium-modified montmorillonite for disinfection of drinking water. *Applied Clay Science* 127–128. 95–104..

Kuila, T., Bose, S., Mishra, A. K., Khanra, P., Kim, N. K., and Lee, J. H. 2012. Effect of functionalized graphene on the physical properties of linear low density polyethylene nanocomposites. *Polymer Testing* 31 31–38.

Landry, V., Blanchet, P., and Boivin, G. 2013. Metal oxide sol-gels (ZrO_2, AlO(OH), and SiO_2) to improve the mechanical performance of wood substrates. *Journal of Nanoparticles* 2013: 1–8.

Lanje, A. S., Sharma, S. J., Ningthoujam, R. S., Ahn, J. S., and Pode, R. B. 2013. Low temperature dielectric studies of zinc oxide (ZnO) nanoparticles prepared by precipitation method. *Advanced Powder Technology* 24 331–35.

Lekha, P. Mtibe, A., Motaung, T. E., Andrew, J. E., Sithole, B. B., and Giblil, M. 2016. Effect of mechanical treatment on properties of cellulose nanofibrils produced from bleached hardwood and softwood pulps. *Maderas. Ciencia y tecnología* 18 457–466.

Li, B., Xu, W., Kronlund, D., Määttänen, A., Liu, J., Smått, J. H., Peltonen, J., Willför, S., Mu, X., and Xu, C. 2015. Cellulose nanocrystals prepared via formic acid hydrolysis

followed by TEMPO-mediated oxidation. *Carbohydrate Polymers* 133. 605–12.

Li, R., Fei, J., Cai, Y., Li, Y., Feng, J., and Yao, J 2009. Cellulose whiskers extracted from mulberry: A novel biomass production. *Carbohydrate Polymers* 76 94–99.

Liang, G., Xu, J., Bao, S., and Xu, W. 2004. Polyethylene/maleic anhydride grafted polyethylene/organic-montmorillonite nanocomposites. I. Preparation, microstructure, and mechanical properties. *Journal of Applied Polymer Science* 91 3974–3980.

Liu, J. 2017. Graphene-based composites for electrochemical energy storage. 1–144. doi:10.1007/978-981-10-3388-9.

Lodha, A., Lodh,a M., Patel, A., Chaudhuri, J., Dalal, J., Edwards, M., and Douroumis, D. 2012. Synthesis of mesoporous silica nanoparticles and drug loading of poorly water soluble drug cyclosporin A. *Journal of Pharmacy and Bioallied Sciences* 4 S92–S94.

Lu, X., Yu, M., Huang, H., and Ruoff, R. S. 1999. Tailoring graphite with the goal of achieving single sheets. *Nanotechnology* 10 269–272.

Malas, A., Pal, P., and Das, C. K. 2014. Effect of expanded graphite and modified graphite flakes on the physical and thermo-mechanical properties of styrene butadiene rubber/polybutadiene rubber (SBR/BR) blends. *Materials and Design* 55. 664–673.

Malwitz, M. M., Lin-Gibson, S., Hobbie, E. K., Butler, P. D., and Schmidt, G. 2003. Orientation of platelets in multilayered nanocomposite polymer films. *Journal of Polymer Science, Part B: Polymer Physics* 41 3237–3248.

Maria, K. H., and Mieno, T., 2015. Synthesis of single-walled carbon nanotubes by low-frequency bipolar pulsed arc discharge method. *Vacuum* 113. 11–18.

Maruyama, T., Kozawa, A., Saida, T., Naritsuka,S., and Iijima, S. 2017. Low temperature Growth of single-walled carbon nanotubes from Rh Catalysts. *Carbon* 116. 128–132.

Mathew, A. P., Oksman, K., Karim, Z., Liu, P., Khan, S. A., and Naseri, N. 2014. Process scale up and characterization of wood cellulose nanocrystals hydrolysed using bioethanol pilot plant. *Industrial Crops and Products* 58 212–219.

Messori, M., Bignotti, F., Santis, R., and Taurino, R. 2009. Modification of isoprene rubber by in situ Silica generation. *Polymer International* 58 880–887.

Meysami, S.S., Koós, A. A., Dillon, F., Dutta, M., and Grobert, N. 2015. Aerosol-assisted chemical vapour deposition synthesis of multi-wall carbon nanotubes: III. Towards upscaling. *Carbon* 88: 148–156.

Mochane, M. J., and Luyt, A. S. 2015. Synergistic effect of expanded graphite, diammonium phosphate and cloisite 15A on flame retardant properties of EVA and EVA/wax phase-change blends. *Journal of Materials Science* 50 3485–3494.

Mochane, M. J., and Luyt, A. S. 2014. Thermal and mechanical properties of polyolefins/Wax PCM blends prepared with and without expanded graphite. University of Free State 1–146 .

Al-Zanganawee J., Moise, C., Katona, A., Bojin, D., and Enachescu, M. 2015. Characterization of single wall carbon nanotubes synthesized by krf excimer laser ablation in nitrogen atmosphere. *Digest Journal of Nanomaterials and Biostructures* 10 1119–1127.

Mokhena, T. C., and Luyt, A. S. 2014. Investigation of polyethylene/sisal whiskers nanocomposites prepared under different conditions. *Polymer Composites* 35 2221–2233.

Mokhena, T. C., and Luyt, A. S. 2017. Electrospun alginate nanofibres impregnated with silver nanoparticles: Preparation, morphology and antibacterial properties. *Carbohydrate Polymers* 165 304–312.

Mokhothu, T. H., Luyt, A. S., and Messori, M. 2014a. Preparation and characterization of EPDM/silica nanocomposites prepared through non-hydrolytic sol-gel method in the absence and presence of a coupling agent. *Express Polymer Letters* 8 809–822.

Mokhothu, T. H., Luyt, A. S., and Messori, M. 2014b. "Reinforcement of EPDM rubber with in situ generated silica particles in the presence of a coupling agent via a sol-gel route. *Polymer Testing* 33. 97–106.

Möller, K., and Bein, T. 2017. Talented mesoporous silica nanoparticles. *Chemistry of Materials* 29 371–388.

Morselli, D., Bondioli, F., Fiorini, M., and Messori, M. 2012. Poly(methyl methacrylate)-TiO_2 nanocomposites obtained by non-hydrolytic sol-gel synthesis: The innovative tert-

butyl alcohol route. *Journal of Materials Science* 47 7003–7012.

Morselli, D., Bondioli, F., Luyt, A. S., Mokhothu, T. H., and Messori, M. 2013. Preparation and characterization of EPDM rubber modified with in situ generated silica." *Journal of Applied Polymer Science* 128 2525–2532.

Morselli, D., Bondioli, F., Sangermano, M., and Messori, M. 2012. Photo-cured epoxy networks reinforced with TiO_2 in-situ generated by means of non-hydrolytic sol-gel process. *Polymer* 53 283–290.

Motaung, T. E., and Mtibe A. 2015. Alkali treatment and cellulose nanowhiskers Extracted from maize stalk residues. *Materials Sciences and Applications* 6 1022–1032.

Mtibe, A., Linganiso, L. Z., Mathew, A. P., Oksman K., John, M. J., and Anandjiwala, R. D. 2015. A Comparative study on properties of micro and nanopapers produced from cellulose and cellulose Nanofibres. *Carbohydrate Polymers* 118. 1–8.

Mtibe, A., Mandlevu, Y., Linganiso, L. Z., and Anandjiwala, R. D. 2015. "Extraction of cellulose nanowhiskers from flax fibres and their reinforcing effect on poly(Furfuryl) alcohol. *Journal of Biobased Materials and Bioenergy* 9 309–317.

Mubarak, N. M., Abdullah, E. C., Jayakumar, N. S., and Sahu, J. N. 2014. An overview on methods for the production of carbon nanotubes. *Journal of Industrial and Engineering Chemistry* 20 1186–1197.

Nagarajan, S., and Kuppusamy, A. K. 2013. Extracellular synthesis of zinc oxide nanoparticle using seaweeds of gulf of mannar, India. *Journal of Nanobiotechnology* 11 1–11.

Nakkala, J. R., Mata, R., and Sadras, S. R. 2017. Green synthesized nano silver: synthesis, physicochemical profiling, antibacterial, anticancer activities and aiological in vivo toxicity. *Journal of Colloid and Interface Science* 499 33–45.

Nava, O. J., Luque, P. A., Gómez-Gutiérrez, C. M., Vilchis-Nestor, A. R., Castro-Beltrán, A., Mota-González, M. L., and Olivas, A. 2017. Influence of camellia sinensis extract on zinc oxide nanoparticle green synthesis. *Journal of Molecular Structure* 1134: 121–25.

Neha, B., Manjula, K. S., Srinivasulu, B., and Subhas, S. C. 2012. Synthesis and characterization of exfoliated graphite/ABS composites. *Open Journal of Organic*

Polymer Materials 2 74–78.

Neto, W. P. F., Silvério, H. A., Dantas, N. O., and Pasquini, D. 2013. Extraction and characterization of cellulose nanocrystals from agro-industrial residue-soy hulls. *Industrial Crops and Products* 42 480–488.

Niederberger, M. 2009. "Aqueous and nonaqueous sol-gel." *Metal Oxide Nanoparticles in Organic Solvents, Synthesis, Formation, Assembly and Applications* 1–13. doi:bfm:978-1-84882-671-7/1.

Novoselov, K. S., Geim, A. K., Morozov, S.V., Jiang, D., Zhang, Y., Dubonos, S. V., Grigorieva, I. V., and Firsov A. A. 2004. Electric field effect in atomically thin carbon films. *Science* 306: 666–669.

Novoselov, K. S., Jiang, D., Schedin, F., Booth, T. J., Khotkevich, V. V., Morozov, S. V., and Geim, A. K. 2005. Two-dimensional atomic crystals. *Proceedings of the National Academy of Sciences* 102 10451–10453.

Pang, X. Y., Song, M. K., Tian, Y., and Duan, M. W. 2012. Preparation of high dilatability expandable graphite and its flame retardancy for LLDPE. *Journal of the Chilean Chemical Society* 57 1318–1322.

Paderni, K., Morselli, D., Bondioli, F., Luyt, A. S., Mokhothu, T. H., and Messori, M. 2014. EPDM rubber reinforced with titania generated by nonhydrolytic sol-gel process. *Polymer Engineering and Science* 54: 2544–2552.

Paul, B., Vadivel, S., Dhar, S. S., Debbarma, S., and Kumaravel, M. 2017. One-pot green synthesis of zinc oxide nano rice and its application as sonocatalyst for degradation of organic dye and synthesis of 2-Benzimidazole derivatives. *Journal of Physics and Chemistry of Solids* 104 152–159.

Paul, D. R., and Robeson, L. M. 2008. Polymer nanotechnology: Nanocomposites. *Polymer* 49 3187–3204.

Qing, Y., Sabo, R., Zhu, J. Y., Agarwal, U., Cai, Z., and Wu, Y. 2013. A Comparative study of cellulose nanofibrils disintegrated via multiple processing approaches. *Carbohydrate Polymers* 97 226–234.

Rao, A. V., Latthe, S. S., Mahadik, S. A., and Kappenstein, C. 2011. Mechanically stable and

corrosion resistant superhydrophobic sol-gel coatings on copper substrate. *Applied Surface Science* 257 5772–5776.

Saha, J., Roy, A. D., Dey, D., Bhattacharjee, D., Paul, P. K., Das, R., and Hussain, S.A. 2017. Effect of zinc oxide nanoparticle on fluorescence resonance energy transfer between fluorescein and rhodamine 6G. *Spectrochimica Acta- Part A: Molecular and Biomolecular Spectroscopy* 175. 110–116..

Salari, Z., Ameri, A., Forootanfar, H., Adeli-Sardou, M., Jafari, M., Mehrabani, M., and Shakibaie. M. 2017. Microwave-assisted biosynthesis of zinc nanoparticles and their cytotoxic and antioxidant activity. *Journal of Trace Elements in Medicine and Biology* 39. 116–123.

Salem, W., Leitner, D. R., Zingl, F. G., Schratter, G., Prassl, R., Goessler, W., Reidl, J., and Schild, S. 2015. Antibacterial activity of silver and zinc nanoparticles against vibrio cholerae and enterotoxic escherichia coli." *International Journal of Medical Microbiology* 305 (1). 85–95.

Saoud, K., Alsoubaihi, R., Bensalah, N., Bora, T., Bertino, M., and Dutta, J. 2015. Synthesis of supported silver nano-spheres on zinc oxide nanorods for visible light photocatalytic applications. *Materials Research Bulletin* 63. 134–140.

Satyamurthy, P., Jain, P., Balasubramanya, R. H., and Vigneshwaran, N. 2011. Preparation andcharacterization of cellulose nanowhiskers from cotton fibres by controlled microbial hydrolysis. *Carbohydrate Polymers* 83 122–129.

Sedira, S., Ayachi, A. A., Lakehal, S., Fateh, M., and Achour. S. 2014. Silver nanoparticles in combination with acetic acid and zinc oxide quantum dots for antibacterial activities improvement—A comparative study. *Applied Surface Science* 311. 659–665.

Shankar, S., and Rhim, J. W. 2017. Facile approach for large-scale production of metal and metal oxide nanoparticles and preparation of antibacterial cotton pads. *Carbohydrate Polymers* 163. 137–145.

Sharma, R. K., and Ghose, R. 2015. Synthesis of zinc oxide nanoparticles by homogeneous precipitation method and its application in antifungal activity against Candida Albicans. *Ceramics International* 41 967–75.

Sibeko M. A., and Luyt A. S. 2013. Preparation and characterization of vinylsilane crosslinked high-density polyethylene composites filled with nanoclay. *Polymer Composites* 34 1720–1727.

Sibeko, M. A., and Luyt A. S. 2014. Preparation and characterisation of vinylsilane crosslinked low-density polyethylene composites filled with nano clays. *Polymer Bulletin* 71 637–657.

Silva, B. L., Nack, F. C., Lepienski, C. M., Coelho, L. A. F., and Becker, D. 2014. Influence of intercalation methods in properties of clay and carbon nanotube and high density polyethylene nanocomposites. *Materials Research* 17 1628–3166.

Silvério, H. A., Neto, W. P. F., Noélio Dantas, N. O., and Pasquini, D. 2013. Extraction and characterization of cellulose nanocrystals from corncob for application as reinforcing agent in nanocomposites. *Industrial Crops and Products* 44. 427–436.

Singh, G. P. B., Baburao, C., Pispati, V., Pathipati, H., Muthy, N., Prassana, S. R. V., and Rathode, B. G. 2012. Carbon nanotubes– a novel drug delivery system. *International Journal of Research in Pharmacy and Chemistry* 2 523–532.

Singh, S., Gaikwad, K. K., Park, S., and Lee, Y. S. 2017. Microwave-assisted step reduced extraction of seaweed (Gelidiella Aceroso) cellulose nanocrystals." *International Journal of Biological Macromolecules* 99. 506–510.

Sirelkhatim, A., Mahmud, S., Seeni, A., Kaus, N. H. M., Ann, L. C., Bakhori, S. K. M., Hasan, H., and Mohamad, D. 2015. Review on zinc oxide nanoparticles: Antibacterial activity and toxicity mechanism. *Nano-Micro Letters* 7 219–242.

Sithara, R., Selvakumar, P., Arun, C., Anandan, S., and Sivashanmugam, P. 2017. Economical synthesis of silver nanoparticles using leaf extract of Acalypha Hispida and its application in the detection of Mn(II) ions. *Journal of Advanced Research* 8 561–568.

Song, P., Cao, Z., Cai, Y., Zhao, L., Fang, Z., and Fu, S. 2011. Fabrication of exfoliated graphene-based polypropylene nanocomposites with enhanced mechanical and thermal properties. *Polymer* 52 4001–4010.

Strawhecker, K. E., and Manias, E. 2000. Structure and properties of poly(vinyl alcohol)/Na+

montmorillonite nanocomposites. *Chemistry of Materials* 12 2943–2949.

Styskalik, A., Skoda, D., Barnes, C., and Pinkas, J. 2017. The power of non-hydrolytic sol-gel chemistry: A review. *Catalysts* 7 1–42.

Su, Y., Wei, H., Li, T., Geng, H., and Zhang, Y. 2014. Low-cost synthesis of single-walled carbon nanotubes by low-pressure air arc discharge. *Materials Research Bulletin* 50 23–25.

Teixeira, R. S. S., Silva, A. S. A., Jang, J. H., Kim, H. W., Ishikawa, K., Endo, T., Lee, S. H., and Bon, E. P. S. 2015. Combining biomass wet disk milling and endoglucanase/β-glucosidase hydrolysis for the production of cellulose nanocrystals. *Carbohydrate Polymers* 128. 75–81.

Thakkar, K. N., Mhatre, S. S., and Parikh, R. Y. 2010. Biological synthesis of metallic nanoparticles. *Nanomedicine: Nanotechnology, Biology, and Medicine* 6 257–262.

Uhl, F. M., Yao, Q., Nakajima, H., Manias, E., and Wilkie, C. A. 2005. Expandable graphite/polyamide-6 nanocomposites. *Polymer Degradation and Stability* 89 70–84.

Valapa, R. B., Pugazhenthi, G., and Katiyar, V. 2015. Effect of graphene content on the properties of poly(lactic acid) nanocomposites. *Royal Society of Chemistry* 5 28410–28423.

Wang, J., Manga, K. K., Bao, Q., and Loh, K. P. 2011. High-yield synthesis of few-layer graphene flakes through electrochemical expansion of graphite in propylene carbonate electrolyte.” *Journal of the American Chemical Society* 133 8888–8891.

Wu, C., Nahil, M. A., Miskolczi, N., Huang, J., and Williams, P. T. 2014. Processing real-world waste plastics by pyrolysis-reforming for hydrogen and high-value carbon nanotubes. *Environmental Science and Technology* 48 819–826.

Xu, L., Zhuang, W., Xu, B., and Cai, Z. 2011. Fabrication of superhydrophobic cotton fabrics by silica hydrosol and hydrophobization. *Applied Surface Science* 257 5491–5498.

Yasmin, A., Luo, J. J., and Daniel, I. M. 2006. Processing of expanded graphite reinforced polymer nanocomposites. *Composites Science and Technology* 66 1179–1186.

Yathisha, R. O., Nayaka, Y. A., and Vidyasagar C. C. 2016. Microwave combustion

synthesis of hexagonal prism shaped ZnO nanoparticles and effect of Cr on structural, optical and electrical properties of ZnO nanoparticles. *Materials Chemistry and Physics* 181. 167–175.

Yousefi, H., Faezipour, M., Hedjazi, S., Mousavi, M. M., Azusa, Y., and Heidari, A. H. 2013. "Comparative study of paper and nanopaper properties prepared from bacterial cellulose nanofibers and fibers/ground cellulose nanofibers of canola straw. *Industrial Crops and Products* 43. 732–737.

Zabihi, O., Ahmadi, M., Abdollahi, T., Nikafshar, S., and Naebe, M. 2017. Collision-induced activation: towards industrially scalable approach to graphite nanoplatelets functionalization for superior polymer nanocomposites. *Scientific Reports* 7 1–13.

Zhang, G., Wang, F., Dai, J., and Huang, Z. 2016. Effect of functionalization of graphene nanoplatelets on the mechanical and thermal properties of silicone rubber composites." *Materials* 9 1–13.

Zhang, Y., Small, J. P., Pontius, W. V., and Kim, P. 2005. Fabrication and electric-field-dependent transport measurements of mesoscopic graphite devices. *Applied Physics Letters* 86 1–3.

Zhao, X., Ohkohchi, M., Inoue, S., Suzuki, T., Kadoya, T., and Ando, Y. 2006. Large-scale purification of single-wall carbon nanotubes prepared by electric arc discharge. *Diamond and Related Materials* 15 1098–1102.